Colloidal Semiconductor Nanoparticles as Functional Materials: Design, Assembly and Applications

Habilitationsschrift

vorgelegt

dem Bereich Mathematik und Naturwissenschaften
der Technischen Universität Dresden

von

Dr. Vladimir Lesnyak
geboren am 28.08.1977 in Kobrin (Belarus)

Eingereicht am: _____

Die Habilitationsschrift wurde in der Zeit von 05/2017 bis 02/2019 im Institut für Physikalische Chemie angefertigt.

PREFACE

This work summarizes results of about ten years of the author's own research activities in the field of colloidal synthesis of semiconductor nanoparticles, their postsynthetic chemical modification, assembly, and applications. I attempted to provide a concise yet comprehensive overview presenting my own results as a part of the knowledge framework created in close collaboration with many colleagues from all over the world. This habilitation thesis consists of an introduction, explaining the motivation of the research accomplished, followed by a main part which briefly presents key achievements of the author with links to appropriate annexes, i.e. original published articles in peer review journals which are attached to this cumulative script, and completed by conclusions.

CONTENT

LIST OF ABBREVIATIONS

AIS	$AgInS_2$ or Ag–In–S with varied composition
CE	cation exchange
CIS	$CuInS_2$ or Cu–In–S with varied composition
CISe	$CuInSe_2$ or Cu–In–Se with varied composition
CTSe	Cu–Sn–Se with varied composition
CZIS	Cu–Zn–In–Se with varied composition
CZSe	Cu–Zn–Se with varied composition
CZTSeS	$Cu_2ZnSnSe(S)_4$ or Cu–Zn–Sn–Se–S with varied composition
DDT	1-dodecanethiol
DFT	density functional theory
ITO	indium tin oxide
LIB	lithium ion battery
LSPR	localized surface plasmon resonance
NC	nanocrystal
NS	nanosheet
OlAm	oleylamine
PEG	polyethylene glycol
mPEG-SH	thiolated methoxypolyethylene glycol
PL	photoluminescence
PLQY	photoluminescence quantum yield
QD	quantum dot
SEM	scanning electron microscopy
(HR)TEM	(high resolution) transmission electron microscopy
TGA	thioglycolic acid
Tz	tetrazole
$5HSCH_2Tz$	5-mercaptomethyltetrazole
UV	ultraviolet
XPS	X-ray photoelectron spectroscopy
XRD	X-ray diffraction

1. INTRODUCTION

Colloidal semiconductor nanocrystals (NCs) or quantum dots (QDs) have evolved during the last few decades from fundamental theoretical concepts to real commercial products owing to intensive efforts by a plethora of research groups worldwide. One of the latest and probably most fascinating examples of commercialization of QDs is a line-up of Samsung QLED TVs, in which QDs are employed as color converters. These nanomaterials benefit on one hand from their unique size-dependent optoelectronic properties, based on the quantum confinement effect.[1] Thus, QDs exhibit extremely attractive optical features, such as widely tunable absorption spectra extending over a broad wavelength range, high photoluminescence (PL) quantum yields (QYs), narrow PL spectral bandwidth, and high thermal and photochemical stability.[2-3] On the other hand, their solution-based synthesis is a remarkably simple process that can be implemented in nearly any moderately equipped chemical laboratory. A typical setup for the so called hot-injection synthesis of semiconductor NCs is presented in *Figure 1a*. High quality materials can be produced by this method at surprisingly low cost. Both these factors greatly promote the investigation of semiconductor NCs, making this field truly interdisciplinary.
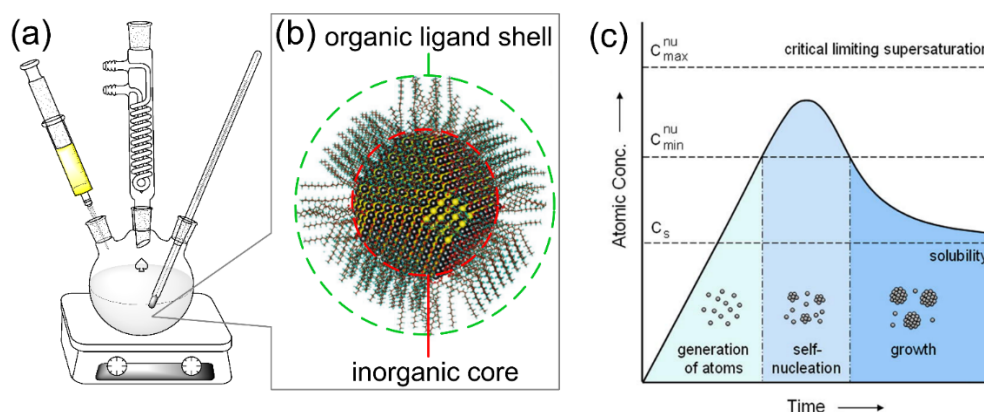

Figure 1. (a) A common setup for the hot-injection synthesis of semiconductor NCs. (b) Calculated atomic structure of a 5 nm sized PbS NC capped with oleic acid. (c) LaMer diagram depicting the concentration variation during the nucleation and the growth of NCs. Reproduced from refs.[4-5]. Copyright 2014 and 2009, AAAS and Wiley VCH Verlag GmbH & Co.

Despite its simplicity, the colloidal synthesis of nanoparticles in its current state allows us to prepare NCs from a wide variety of semiconductors, mainly of the II-VI, IV-VI, III-V, I-III-VI, I-II-IV-VI and I-IV-VII families (corresponding examples are CdSe, PbS, InP, CuInS$_2$, Cu$_2$ZnSnS$_4$, and CsPbBr$_3$). Furthermore, manipulating the conditions of the synthesis makes it possible to tune the size of these particles, their shape, and crystal structure. Moreover, one can combine two or more semiconductors in one nano-object with different design, such as alloys and heterostructures (core/shell, Janus-type, segmented particles). The surface chemistry of these NCs can also be adjusted by means of post-synthetic functionalization and ligand exchange. The first is very important for the biomedical application of nanoparticles, the latter is of paramount importance for their integration into optoelectronic devices.[2, 6-14] Thus, complex chemistry and physics undergird these apparently simple materials. Being soluble objects, these nanomaterials can be processed via common solution-based techniques, such as drop-casting, spin- and spray-coating, as well as inkjet-printing. Most of their optoelectronic applications, e.g. in light-emitting diodes (LEDs), solar cells, photodetectors, and field-effect transistors, involve NCs in the form of solid thin films.

A typical structure of a semiconductor nanoparticle shown in *Figure 1b* consists of an inorganic core and an organic shell of stabilizing ligands providing them solubility in a variety of solvents and stability against aggregation. In the colloidal synthesis, suitable molecular precursors (mainly inorganic salts or organometallic compounds) are reacted in a liquid medium in the presence of appropriate ligands.[15] Chemical reactions between the precursors release reactive species, called monomers which are responsible for further nucleation and growth of nanoparticles.[16-22] In this process, the reaction conditions of the colloidal synthesis have to be carefully controlled to produce monodisperse particles. In particular, it is important to temporally separate the nucleation and the growth in order to achieve a narrow size distribution of the NCs.[23-25] This is generally implemented by tuning the rate at which the reactive species are released from corresponding precursors. The LaMer diagram in *Figure 1c* shows the evolution of the concentration in the formation of monodisperse NCs demarcating the three stages: 1) generation of atoms (or other active species), i.e. the monomer formation, 2) the nucleation when the concentration of the monomers reaches a certain minimal value (nucleation threshold), and 3) the growth of the formed nuclei by consumption of the monomer species in the solution.[26]

Since the author has contributed to different fields of research on semiconductor NCs, this thesis presents three main blocks of results obtained in developing design of the NCs, their assembly and potential applications. The design includes a direct synthesis of the NCs either in aqueous or in organic media, as well as postsynthetic adjustment of the NC cores and their surface via cation and ligand exchange, respectively. The main aims of this work were to prepare complex alloyed (mixed) and heterostructured NCs with well controllable properties, in particular size, shape, composition, crystal structure, and surface chemistry. Among these main characteristics of the NCs, their size, shape, composition, and to some extent crystal structure define optical and electronic features of the materials, whereas the surface chemistry offers many approaches to functionalize the NCs via e.g. ligand shell modification, exchange or even complete removal. Using technique of aqueous colloidal synthesis, we developed methods to prepare several types of alloyed semiconductor NCs, such as $Zn_{1-x}Cd_xSe$,[27] $ZnSe_{1-x}Te_x$,[28] $Cd_{1-x}Hg_xTe$[29] exhibiting strong fluorescence in the blue and near-infrared (NIR) regions of the spectrum. Later work on Cd(Hg)-free NCs has resulted in aqueous Ag–In–S-based nanoparticles, possessing strong fluorescence in the visible region.[30] These materials appended the library of available aqueous QDs and extended their optical properties, in particular their PL.[31] As a part of the NC design, we developed a convenient approach to a partial cation exchange (CE) of pre-synthesized copper chalcogenide nanoparticles[32] towards complex multinary Cu–Zn–In–S,[33] Cu–Zn–In–Se,[34] Cu–Zn–Sn–Se,[35] as well as to heterostructured Cu_2Se–CdSe and Cu_2Se–ZnSe NCs[36].

From the point of view of the new NC surface chemistry, we introduced novel tetrazole (Tz)-capping of semiconductor NCs, which allows for a controllable complexation of the particles via a simple addition of different cations to their colloidal solutions.[37-40] Furthermore, we developed amphiphilic Au[41] and CdTe[42-43] nanoparticles by employing a specially designed short-chain polyethylene glycol molecules functionalized with –SH group. These particles were demonstrated to be capable of a spontaneous transport through model and cellular membranes,[43] that is of particular interest for studying intracellular transport phenomena and for further bio-labelling applications of these materials. Later on, we used a technique of the ligand exchange toward all-inorganic capping in order to precisely engineer QD shells via alternation of ZnS and CdS monolayers in colloidal ionic layer deposition.[44]

Tz-based unique surface coverage has led to the development of highly porous non-ordered 3D assemblies of nanoparticles in the forms of gels and aerogels.[37-40] In these structures NCs were bridged via metal ions forming strong complexes with Tz-molecules. A similar approach to networking

semiconductor NCs has been applied to inorganically capped particles resulting in all-inorganic NC (aero)gels, a promising material for photocatalysis.[45]

Thus developed materials and approaches have been tested for application in several different fields. For instance, copper selenide nanoparticles and nanosheets (NSs) were applied as conductive coatings, in which the NSs exhibited remarkably better performance, than contending nanoparticles, being deposited in the form of thin films on flexible substrates.[46] Another simple binary copper chalcogenide, CuS, synthesized in the form of hierarchical superstructures built of NCs, has been successfully applied in lithium ion batteries (LIBs) as an electrode material.[47] $Cu_{2-x}Se$ NCs have been employed as a material that can switch its localized surface plasmon resonance (LSPR), thus resulting in well-controllable transmittance of a simple device in the NIR region, which can be easily tuned electrochemically.[48] Furthermore, fluorescent Cu–Zn–In–S-based QDs were incorporated into polymer matrices forming photostable composites, which hold a great potential for application in photovoltaic windows.[49-50]

2. MAIN RESULTS

2.1. Design

Design of semiconductor NCs summarized in this section includes: 1) their direct synthesis either in aqueous or in organic media, 2) postsynthetic modification of their surface via ligand exchange, and 3) postsynthetic modification of their cores by means of CE.

2.1.1. Alloyed aqueous semiconductor nanocrystals

Main body of work on aqueous synthesis of semiconductor NCs was devoted to CdS[51-52] and to CdTe[31, 53-56]. As these two materials have intrinsic restrictions of their optical properties due to limited tuning of their band gaps via size change during their growth, additional handle would be the formation of alloyed nanoparticles. In these materials band gap can be tuned not only by the size of the NCs, but also by the composition.[57] Following this strategy, by using mixed Cd- and Zn-precursors and a synthetic setup shown in *Figure 2a*, we synthesized $Zn_xCd_{1-x}Se$ QDs with a low cadmium content (x=0.8–1), which subsequently were subjected to photochemical treatment resulted in a dramatic increase of the PL intensity (*Annex 1*).[27] Thus obtained NCs exhibited fluorescence in the UV–blue spectral region with PL maxima ranging from 390 to 460 nm and with PLQYs of 20–30%. The observed shift of the PL maximum upon the irradiation with a powerful white light Xe lamp depended on the Cd content in the particles. An increase of the Cd content in the NCs resulted in a further shift of the PL maximum to longer wavelengths, yet at the same time a decrease of the PL QY was observed. Alternatively, to shift the fluorescence of pure ZnSe QDs toward longer wavelengths, alloying from anion side has been developed that resulted in a facile one-pot synthesis of blue-emitting glutathione-capped $ZnSe_xTe_{1-x}$ NCs possessing PLQYs of up to 20% (*Annex 2*).[28] These nanoparticles were further incorporated into a water dispersed polymer in order to enhance their stability and processability yielding transparent fluorescent inorganic–organic composites. Thus, by these two types of alloyed NCs we covered UV-blue region of the visible spectrum, inaccessible by either pure binary ZnSe or CdTe QDs (*Figure 2b*).
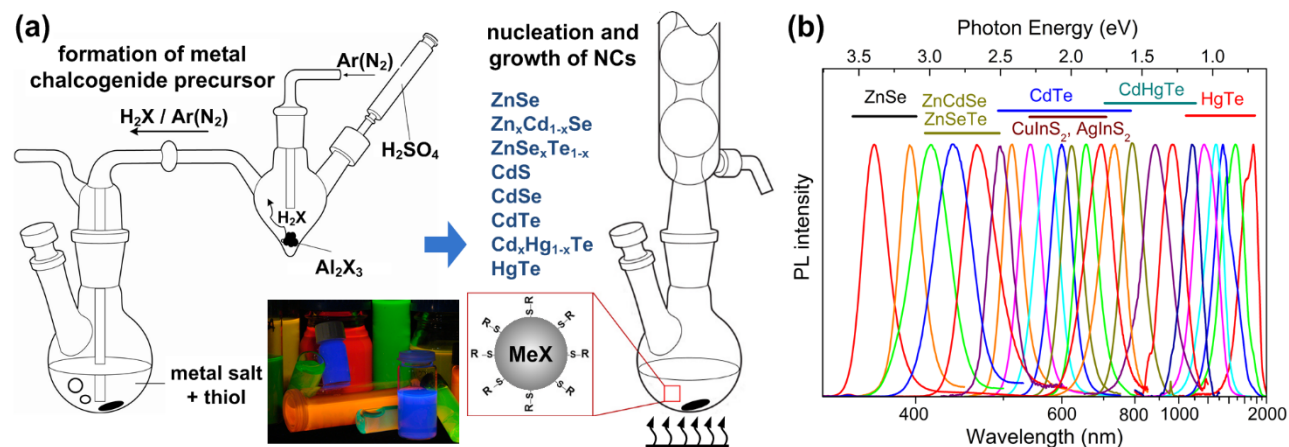

Figure 2. (a) Scheme of a setup for the aqueous synthesis of various metal chalcogenide NCs with a photo of different NC colloids under UV-light excitation. (b) PL spectra of different aqueous QDs. Adapted from ref.[31]. Copyright 2013, the Royal Society of Chemistry.

A similar strategy was applied to push the PL of pure CdTe QDs beyond the visible region, which is basically limited by the bulk ban gap of CdTe (1.56 eV)[58]. In this direct one-pot synthesis we used a mixture of Cd- and Hg-precursors aiming at alloyed $Cd_xHg_{1-x}Te$ QDs with a narrower band gap (*Annex 3*).[29] In this system, moderate variations of the initial Cd^{2+}/Hg^{2+} ratio from 98/2 to 95/5 in the reaction

mixture led to a vast shift of the PL maxima of the resulting products from 640 to 1600 nm. The PL of these alloyed nanoparticles covers the first and the second diagnostic windows and two telecommunication transmission windows at 1.3 and 1.55 μm (*Figure 2b*), making them promising candidates as labels for *in vivo* imaging (when properly encapsulated in a stable matrix to prevent release of Cd and Hg ions) and as optical amplifiers. The high PLQY of these samples with values up to 55% for the red emitting, and up to 60% for the NIR emitting QDs was a clear indication of their excellent quality. We further determined the absolute electronic energy levels in $Cd_xHg_{1-x}Te$ QDs with varying size/volume and Hg content by using cyclic voltammetry measurements and density functional theory (DFT)-based calculations. The electrochemical measurements demonstrated several distinct characteristic features in the form of oxidation and reduction peaks in the voltammograms, where the peak positions were dependent on the volume of the NCs as well as on their composition (*Annex 4*).[59] The volume-dependent shift in the characteristic reduction and oxidation peak potentials was attributed to the alteration in the energetic band positions owing to the quantum confinement effect. We also demonstrated the composition (Cd/Hg=98.3/1.7 and 97.0/3.0)-dependent alteration in the electronic energy levels of $Cd_xHg_{1-x}Te$ NCs for two different samples with similar volumes. Thus obtained electronic energy level values of $Cd_xHg_{1-x}Te$ NCs as a function of volume and composition demonstrated good congruence with the corresponding absorption and emission spectral data supported by DFT-based calculations. The latter revealed that incorporation of Hg into CdTe NCs mostly affects the energy levels of conduction band edge, whereas the valence band edge remains almost unaltered.

The applications of cyclic voltammetry was further extended to *in situ* monitoring of degradation processes in water-soluble CdTe QDs (*Annex 5*).[60] Observed correlations between characteristic features of voltammograms and the PL spectra allowed us to propose mechanisms responsible for evolution of the fluorescence properties as well as degradation pathway of CdTe QDs at low pH. We found that when aqueous thioglycolic acid (TGA)-capped CdTe QDs were introduced into a buffer solution with pH 5, thiolic groups were protonated, and Cd–S bonds on the surface were disrupted, that resulted in the drop of QD stability against oxidation. Nevertheless, TGA molecules remained adsorbed on the Cd-terminated surface of QDs, being anchored to the particle surface by weak van der Waals bonds. Upon oxidation in air, CdTe QDs first lost cadmium, which led to the excess of tellurium that resulted in a PL QY decrease within several minutes. In contrast, in an inert atmosphere PL of QD solutions was retained, although slowly decreasing with time due to a gradual aggregation of the particles and their precipitation from solution.

Despite excellent optoelectronic properties of the above described II-VI nanomaterials, most of them contain toxic elements, such as Cd and Hg, which can be hazardous when released to the environment. That is why their widespread applicability faces serious restrictions. Therefore, nowadays the focus of research on semiconductor NCs has broadened out on copper and silver chalcogenide-based ternary and quaternary compounds, e.g. $CuInS_2$ (CIS), $CuInSe_2$ (CISe), $AgInS_2$ (AIS), Cu_2ZnSnS_4 (CZTS), etc.[61-64] In the framework of this research trend, we developed a facile synthesis of brightly emitting alloyed AIS NCs applying subsequent size-selective precipitation to crude aqueous colloids in order to narrow size distribution of the particles and thus to improve their PL properties (*Annex 6*).[30] In this way we were able to select up to 11 fractions emitting in a broad color gamut from deep-red to bluish-green with the PLQY reaching 47% for intermediate fractions. The size of the isolated AIS QDs varied from ~2 to ~3.5 nm at a roughly constant chemical composition of the particles throughout the fractions. The decrease of the mean particle size in consecutive fractions was accompanied by an increase of the PL bandwidth. Examples of the design of copper chalcogenide-based NCs are presented in **Sections 2.1.4**

and **2.1.5**. *Figure 2b* represents a collection of the PL spectra of different aqueous QDs having different sizes and compositions, which cover a broad spectral range from the UV to the NIR. The main achievements and the state of the art of the aqueous synthesis of semiconductor NCs were summarized in the review (*Annex 7*).[31]

2.1.2. Tetrazole-capped aqueous nanocrystals

Typically aqueous semiconductor NCs are capped by functionalized thiol-containing molecules, such as TGA and mercaptopropionic acid, cysteine, cysteamine, glutathione, etc., which are directly used in the synthesis as stabilizers (ligands) forming complexes with metal cations.[31, 65-66] In order to extend functionality of the NC surface, we introduced a novel ligand, 5-mercaptomethyltetrazole (5-HSCH$_2$Tz) resulting in brightly luminescent water-soluble CdTe QDs with PL QYs of up to 60% (*Annex 8*).[37] Schematic structure of these nanoparticles along with a transmission electron microscopy (TEM) image are displayed in *Figure 3a–b*. In the synthesis 5-HSCH$_2$Tz behaves analogously to the widely used TGA, although stronger complexation affinity of the Tz moiety to Cd^{2+} ions slows down the nucleation and the growth of the NCs. Note that orange–red emission, which corresponds to the size of the NCs equal to 3.3 nm, was reached after almost four days of boiling the reaction mixture (*Figure 3c–d*). At the same time, this strong complexation imparts these NCs a unique ability to form 3D non-ordered highly porous assemblies (gels) upon the addition of metal salts, which will be discussed in **Section 2.2.2**. Similar capping was realized on gold NCs (*Annex 9*)[38] and ZnSe QDs (*Annex 10*)[39], that allowed for fabrication of mixed metal–semiconductor and semiconductor 1–semiconductor 2 assemblies. In the case of 5-HSCH$_2$Tz-capped ZnSe NCs we used the same method of the photochemical treatment as for TGA-capped particles mentioned above[27]. This treatment eventually resulted in the formation of a ZnS-rich shell on the surface of the particles that covers defects acting as trap states for charge carriers generated upon light excitation. Main results published on Tz-based ligands and precursors for nanostructured materials, including our own contribution to this topic, were summarized in a recent review (*Annex 11*).[40]
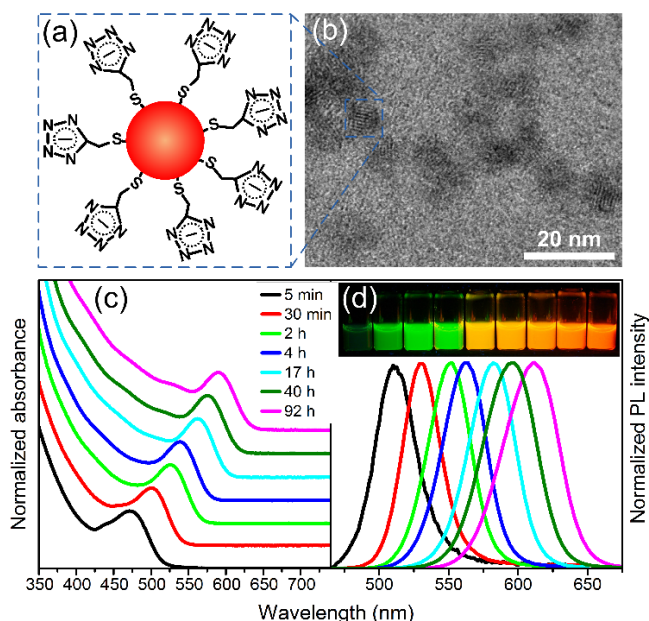

Figure 3. (a) Schematics of a 5-HSCH$_2$Tz-capped CdTe nanoparticle. (b) TEM image of CdTe NCs. Evolution of absorption (c) and PL (d) spectra of 5-HSCH$_2$Tz-capped CdTe NCs during their growth. The inset in (d) shows a photograph of the corresponding fluorescence color change of the NC colloid under UV light. Adapted from ref.[37]. Copyright 2010, American Chemical Society.

2.1.3. Amphiphilic nanocrystals

With the proper design and the fine tuning of their structure, ligands such as thiolated polyethylene glycols (PEGs) enable the synthesis of semiconductor NCs in a variety of solvents. Thus, employing short-chain PEG molecules terminated with –SH group ($H_3C–[O(CH_2)_2]_7–SH$), CdTe NCs schematized in *Figure 4a*, can be synthesized in water, toluene, dimethylacetamide, or in dimethylformamide solution (*Annexes 12, 13*).[42-43] Among them, high-boiling, good coordinating solvents such as dimethylacetamide and dimethylformamide accelerate the growth of the NCs yielding stable colloids, whose which PL maxima can be tuned to cover the region of 540–640 nm with PL QYs of up to 30%.[43] This stabilizer imparts the nanoparticles a unique ability of spontaneous phase transfer between media of different polarity, such as in a simple test experiment shown in *Figure 4b*, where mPEG-SH-caped CdTe QDs being added to a toluene layer poured over water and chloroform layers, start to transfer into water layer after 30 min and further to chloroform after approx. 2 hours.[43] Note that no adjustments of the solvent content such as the addition of some surface-active species are needed to initiate migration of the NCs. Hence, these QDs demonstrate an amphiphilic behavior. The same stabilizer can be applied to synthesize gold NCs, which form stable and highly concentrated colloids (*Annex 14*).[41] These particles are also capable of a similar spontaneous tri-phase transfer owing to their inherent compatibility with media of different polarity.
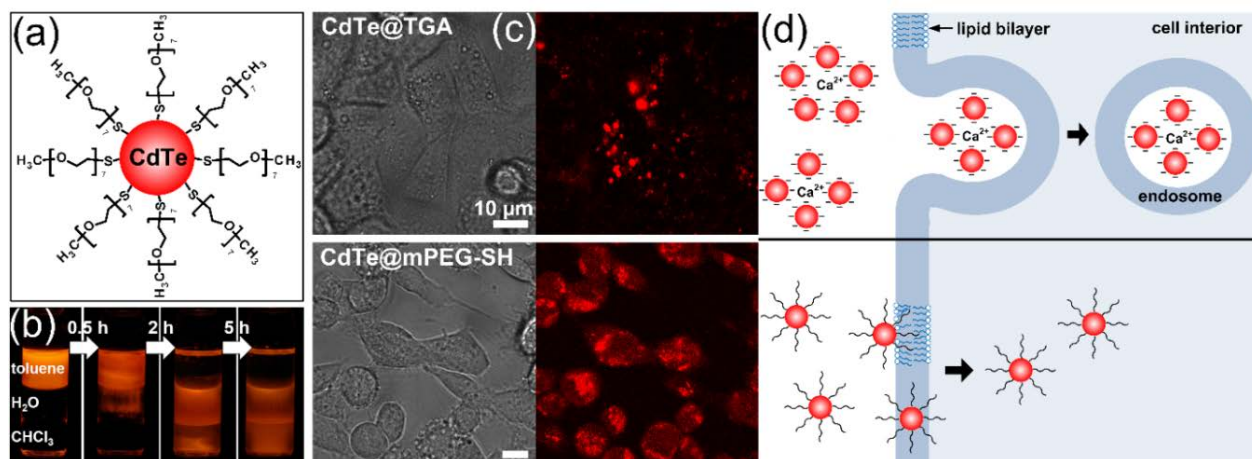

Figure 4. (a) A sketch of a CdTe NC capped by mPEG-SH. (b) Photographs of vials demonstrating the spontaneous tri-phase transfer of mPEG-SH-capped CdTe QDs from toluene through water into chloroform with time, under UV light. (c) Bright field (left panels) and confocal microscopy (right panels) images of live cells acquired after 1 h of incubation in the presence of TGA-capped CdTe (top) and mPEG-SH-capped CdTe (bottom) QDs. (d) Simplified scheme of the penetration of the corresponding QDs into a cell. Adapted from ref.[43]. Copyright 2012, American Chemical Society.

Thus obtained amphiphilic CdTe QDs were further studied in transport processes through lipid bilayers of model (giant unilamellar vesicles and giant plasma membrane spheres) and cellular plasma membranes (*Annex 13*).[43] For the first time it was found that these NCs were able to permeate through the both types of membranes. Furthermore, experiments performed on live cells demonstrated the nonendocytic uptake of these amphiphilic particles, while hydrophilic TGA-capped CdTe QDs were solely accumulated in endosomes, as evidenced by fluorescence confocal microscopy images shown in *Figure 4c* and schematized in *Figure 4d*. This makes the amphiphilic QDs promising agents for tracking whole cells as well as intracellular processes. Moreover, their high colloidal stability in various biological media and robust emission properties can be exploited for a controllable delivery of agents for therapeutic

applications. Most of the results obtained on the synthesis and characterization of amphiphilic NCs were summarized in a recent review.[67]

2.1.4 Synthesis of copper chalcogenide nanocrystals

Another type of semiconductor nanomaterials is coper chalcogenide-based NCs, which typically do not exhibit fluorescence (recently reported PL from copper sulfide NCs is one of a few examples)[68], however many of these compounds possess a strong LSPR.[62, 69-75] Unlike noble metal nanoparticles, exhibiting LSPR owing to a large concentration of free electrons, copper chalcogenide NCs have holes as free carriers, associated with copper vacancies, constituting a class of so called self-doped or degeneratively doped semiconductor nanomaterials. We developed a facile and general approach to synthesize $Cu_{2-x}S$, $Cu_{2-x}Se_yS_{1-y}$, and $Cu_{2-x}Te_yS_{1-y}$ NCs ranging in sizes from 3 to 10 nm (*Annex 15*).[32] This approach has an advantage over the existing ones as it does not involve the hot-injection and does not use phosphines, requires moderate reaction temperatures (200–220 °C), and is easily up-scalable. In fact, scaling up of this synthesis yielded monodisperse nanoparticles without variations in their morphology. Main approaches of large-scale syntheses of nanomaterials were summarized in a recent review (*Annex 16*).[76] Alloyed $Cu_{2-x}Se_yS_{1-y}$ and $Cu_{2-x}Te_yS_{1-y}$ NCs formed due to the incorporation of sulfur by using 1-dodecanethiol (DDT) as a ligand along with oleic acid. Despite their mixed structure, the samples showed optical properties, in particular the position of their plasmon bands, similar to those reported for pure binary copper chalcogenides, i.e., approximately 1800 nm (1270 nm after a prolonged oxidation), 1300, and 800 nm for nonstoichiometric copper sulfide, selenide–sulfide, and telluride–sulfide, respectively. Moreover, these plasmon bands were demonstrated to be widely tunable via a controlled oxidation generating copper vacancies.
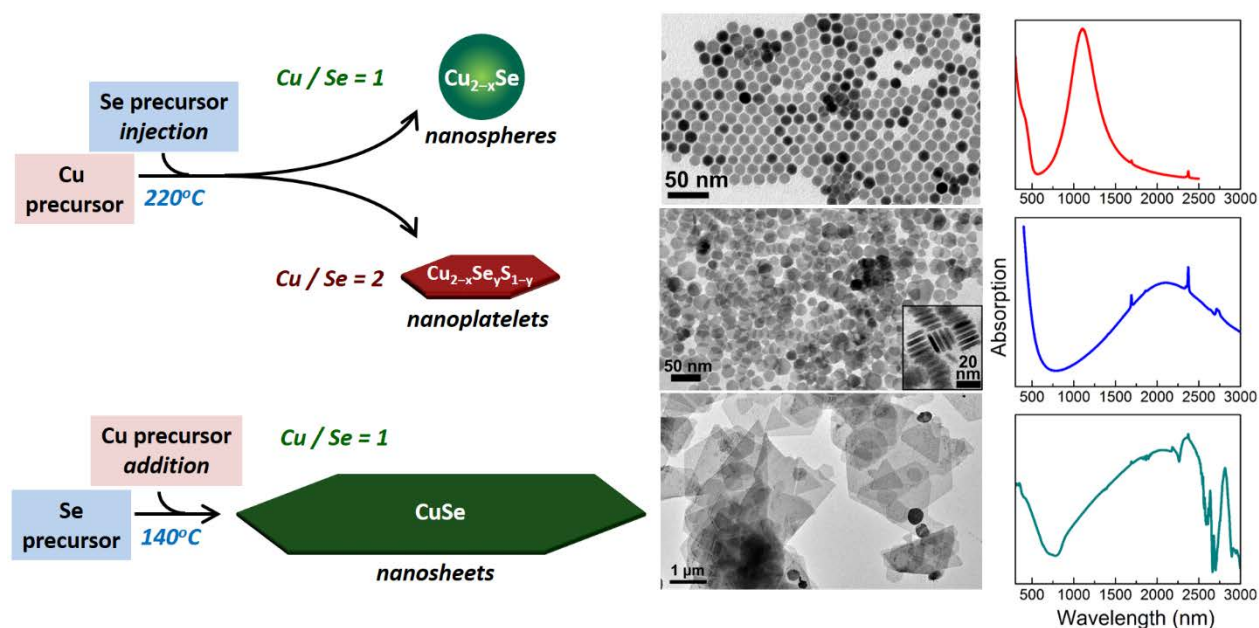

Figure 5. Easy shape control of copper selenide NCs by varying basic reaction parameters: from $Cu_{2-x}Se$ spherical nanoparticles through $Cu_{2-x}Se_yS_{1-y}$ nanoplatelets to large CuSe nanosheets. In all syntheses the same Cu- and Se-precursors were employed. On the right, corresponding TEM images and absorption spectra are shown. Adapted from refs.[35-36, 46]. Copyright 2014, 2015, and 2016, American Chemical Society and Wiley VCH Verlag GmbH & Co.

We further introduced a novel synthesis of copper selenide nanomaterials based on the hot-injection method, in which we achieved a straightforward control of the shape, size, and composition of the resulting NCs via tuning basic reaction conditions, such as temperature, precursor ratio, and

sequence of mixing. Thus, injecting Se-precursor (Se powder dissolved in DDT and oleylamine (OlAm)) into a solution containing Cu-precursor (copper acetylacetonate dispersed in DDT–OlAm mixture) at 220°C resulted in spherical $Cu_{2-x}Se$ NCs, when the ratio between Cu- and Se-precursors was 1 (*Annex 17*),[36] and in hexagonal $Cu_{2-x}Se_yS_{1-y}$ nanoplatelets, when Cu/Se = 2 (*Annex 18*),[35] as summarized in *Figure 5*. Furthermore, adding the Cu-precursor to the Se-precursor at lower reaction temperature (140°C) yielded large CuSe NSs with lateral dimensions of up to 3 μm and thickness of 4–5 nm (*Annex 19*).[46] All these copper selenide nanomaterials possess a strong LSPR in the NIR, as displayed in *Figure 5*.

2.1.5. Cation exchange

Binary and quasi-ternary copper chalcogenide NCs described in **Section 2.1.4** constitute a perfect platform to synthesize more complex multinary (multicomponent) nanomaterials using CE method[77-81]. This technique basically consists in the controllable replacement of host cations in the lattice of NCs with guest cations added in the form of appropriate precursors, studied mainly on the example of metal chalcogenide nanoparticles. This process is governed by both thermodynamic and kinetic factors, such as the difference between the crystal lattice energies (association and dissociation) of the existing and newly forming phases, solvation and desolvation energies of the outgoing and incoming ions, solid-state diffusion of cations, etc. In copper chalcogenide nanoparticles copper ions are very mobile, so they can be easily exchanged with a range of different cations. Exploiting this property we developed a convenient strategy to controllable synthesis of multicomponent compounds based on partial CE, i.e. a partial replacement of Cu^+ ions in the crystal lattice. A general scheme of CE showing main products, which depend on miscibility of host and guest crystal phases, is presented in *Figure 6*. According to this scheme, resulting nanomaterials can be completely or partially cation-exchanged, forming either doped or alloyed (mixed) structures, or heterostructures with a sharp boundary between different phases. The latter can be arranged either in the core/shell or the Janus-like structure.
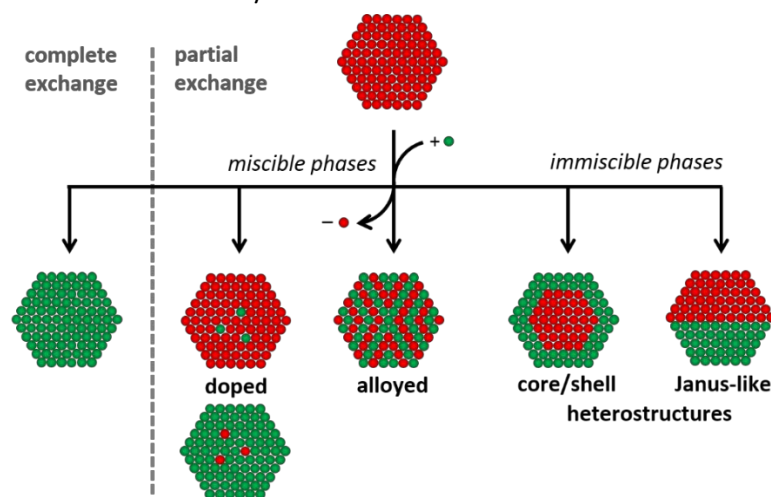

Figure 6. *A general scheme of CE of NCs showing its main products.*

Since the direct synthesis of multinary copper chalcogenide-based NCs involves reaction between several compounds with different reactivity, it is limited in terms of the control over the size, shape, and composition of resulting particles. Therefore, more facile and controllable approach would be the synthesis of simple binary compounds in the first stage with subsequent *in-situ* partial CE towards complex alloy or heterostructures. This strategy was employed to synthesize different ternary and quaternary NCs, such as CIS, CISe, CZSe, CTSe, CZTSe, CZIS, CZISe.[33-35] For example, starting from $Cu_{2-x}Se_yS_{1-y}$ nanoplatelets (see **Section 2.1.4**), we obtained copper zinc (or tin) selenide–sulfide (CZSeS and

CTSeS) and copper zinc tin selenide–sulfide (CZTSeS) particles with approx. 20 nm lateral size (*Annex 18*).[35] In this process, the initial feed ratio of cation precursors (i.e., Zn and/or Sn) to copper ions mediates the final composition of the alloyed compounds without altering the morphology and hexagonal crystal structure of the starting nanoplates. Furthermore, we demonstrated that by the incorporation of guest zinc and tin cations into Se/S anion framework of $Cu_{2-x}Se_yS_{1-y}$ nanoplates, it was possible to engineer the band gap of the resulting alloyed NCs, which opens new opportunities for their application as light absorbers to fabricate solar cells.
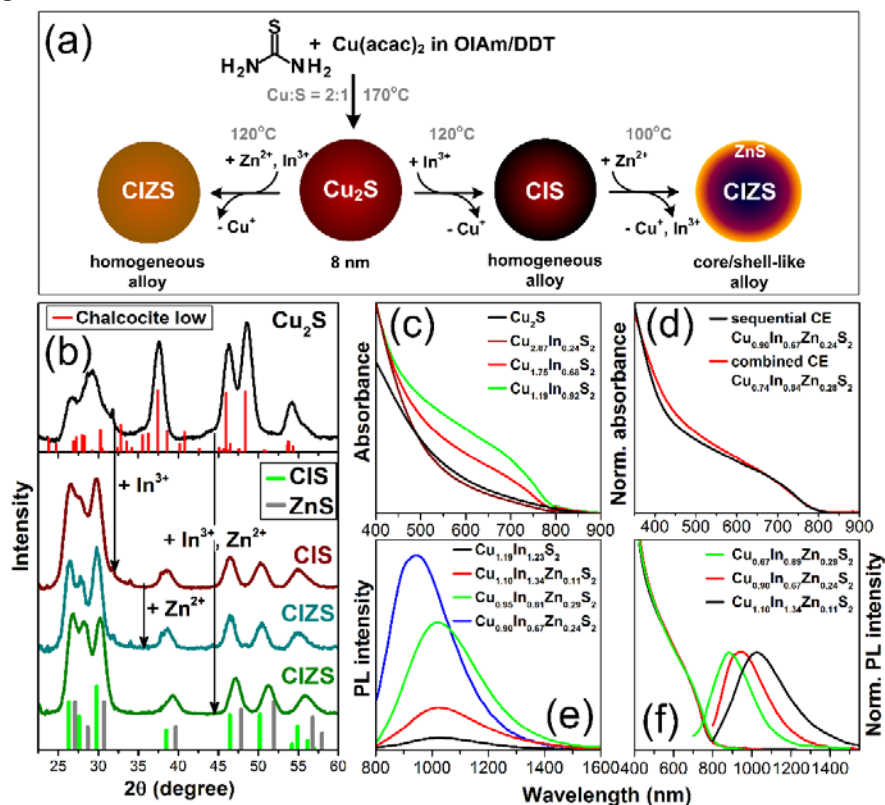

Figure 7. (a) Scheme of the synthesis of pristine Cu_2S NCs and their exchange reactions to CIS and CZIS NCs possessing both homogeneous (left) and core/shell (right) alloy structures. (b) XRD patterns of pristine Cu_2S NCs, exchanged CIS, and CZIS NCs obtained by sequential and simultaneous injection of In- and Zn-precursors. (c) Absorption spectra of parent Cu_2S NCs and exchanged CIS NCs with varied In content. (d) Absorption spectra of CZIS NCs obtained by sequential and combined CE. (e) PL spectra of CZIS NCs with increasing Zn content. (f) Absorption and PL spectra of CIZS NCs with different compositions. Adapted from ref.[33]. Copyright 2015, American Chemical Society.

A similar strategy was utilized to synthesize ternary copper indium sulfide (CIS) and quaternary copper zinc indium sulfide (CZIS) NCs (*Annex 20*).[33] This approach consisted of a three-step sequence: first, binary Cu_2S NCs were synthesized, followed by the homogeneous incorporation of In^{3+} by an *in situ* partial CE reaction, yielding CIS NCs. In the last step, a second CE was performed, where Zn^{2+} partially replaced Cu^+ and In^{3+} ions at the surface, creating a ZnS-rich shell with the preservation of the size and the shape (*Figure 7a*). Alternatively, by combining two precursors (In^{3+} and Zn^{2+}) in one pot, homogeneously alloyed CZIS NCs with higher zinc content were synthesized. Careful tuning reaction parameters (growth and exchange times as well as the initial $Cu^+:In^{3+}:Zn^{2+}$ ratios) allowed us to achieve the precise control over both the size and the composition accompanied by a slight rearrangement of low symmetry monoclinic crystal structure of pristine Cu_2S particles to higher symmetry hexagonal lattice of CIS NCs (*Figure 7b*). We furthermore demonstrated that the sequential exchange with Zn^{2+} led

14

to a sufficient increase of the PL efficiency and that PL could be tuned from 850 to 1030 nm by carefully controlling the Cu:In:Zn content in the NCs (*Figure 7e, f*). On the contrary, homogeneously alloyed CZIS NCs did not exhibit any PL signal, although their absorption spectra were very similar to those of the core/shell (ZnS-surface rich) particles (*Figure 7c, d*). Cytotoxicity tests confirmed the biocompatibility of the synthesized CZIS NCs, which opens up opportunities for their application as NIR fluorescent markers in the biomedical field.

This sequential one-pot approach was further applied to synthesize CISe-based NCs in order to push their PL farther to the NIR region, since CISe has a narrower bulk band gap and a larger Bohr radius than CIS (1.04 eV and 10.6 nm vs. 1.45 eV and 4.1 nm, respectively). In this case, firstly binary highly copper-deficient $Cu_{2-x}Se$ NCs were synthesized (see **Section 2.1.4**), followed by a partial CE of Cu^+ to In^{3+} ions, yielding CISe NCs (*Annex 21*).[34] Subsequently, ZnS shell was grown in the third step, resulting in CISeS/ZnS core/shell particles. The shell growth led to a drastic increase in the size and reshaping the particles from spheres to trigonal pyramids, while preserving their crystal structure. In this process, for the first time, we observed a prominent anion exchange Se^{2-}-to-S^{2-}, whose efficiency was dependent on the size of the core NCs being limited by the surface region. Furthermore, we were able to cover a wide range of the PL maxima from 990 to 1210 nm by varying the particle size, while keeping the spectra relatively narrow for this type of semiconductor nanoparticles. Thus, we were able to push the PL maxima to longer wavelengths with the large CISeS/ZnS NCs exhibiting the farthest for this material emission in the NIR, which goes beyond the bulk band gap of CISe.

As mentioned above, when the host and the guest crystal structures are immiscible, CE yields heterostructured NCs, either core/shell or Janus-like particles (*Figure 6*). The latter were obtained in the Cu^+-to-Cd^{2+} and Cu^+-to-Zn^{2+} CE reactions on copper selenide NCs (*Annex 17*).[36] In particular, in this work we compared the reactivity of stoichiometric Cu_2Se NCs with that of nonstoichiometric $Cu_{2-x}Se$ NCs to gain insights into the mechanism of CE at the nanoscale, as schematized in *Figure 8a*. We have found that the presence of a large density of copper vacancies significantly accelerated the exchange process at room temperature and corroborated vacancy diffusion as one of the main drivers in these reactions. Partially exchanged samples exhibited Janus-like heterostructures made of immiscible domains sharing epitaxial interfaces (*Figure 8b–f*). In the case of Cu^+-to-Cd^{2+} CE it was possible to monitor the transformation by means of the XRD analysis (*Figure 8g*), since Cu_2Se and CdSe have distinctly different crystallographic patterns, unlike the case of Cu_2Se–ZnSe pair. In both systems we observed a drastic difference in the kinetics of the CE between stoichiometric and nonstoichiometric NCs (*Figure 8h*), which revealed that Cu vacancies play a key role in CE reactions involving copper selenide NCs. Furthermore, room temperature conditions were found advantageous compared to higher temperature (150 °C) conditions, owing to the preservation of copper vacancies over time, which resulted in a much more efficient exchange on substoichiometric $Cu_{2-x}Se$ NCs. We also unraveled the multifunctional role of phosphines, like tri-n-octylphosphine, in these reactions, which, besides acting as a selective solvating ligand for Cu^+ ions exiting the NCs during the exchange, also enable anion diffusion, by extracting an appreciable amount of selenium to the solution phase, which may further promote the exchange process. Therefore, the use of NCs with a high density of Cu vacancies can simplify CE reactions and make them more practical, for example, by significantly reducing the ratio between host and guest cations and by working under mild conditions, for example, at room temperature.
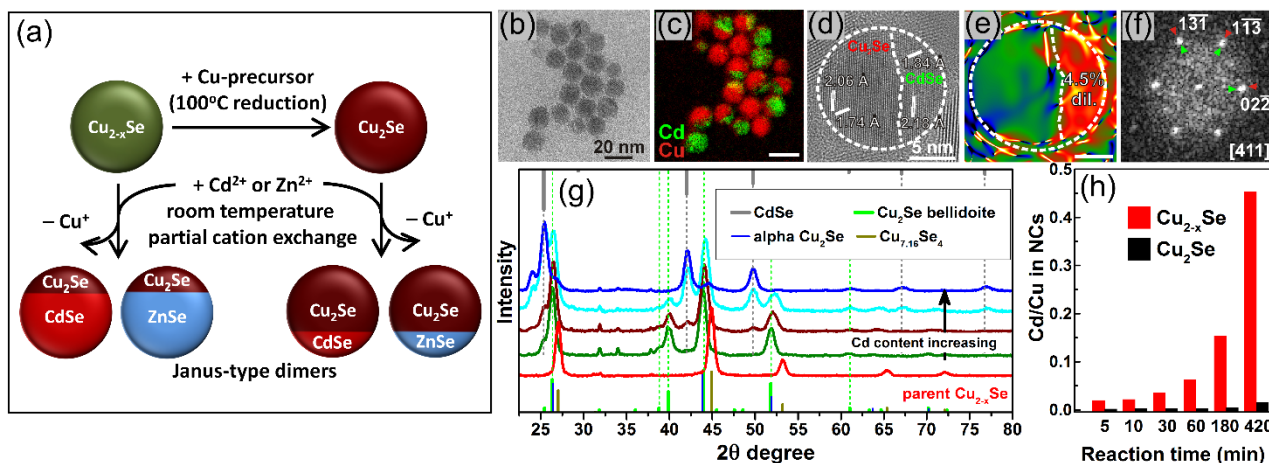
Figure 8. (a) Scheme of the reduction of $Cu_{2-x}Se$ NCs and subsequent CE Cu-to-Cd and Cu-to-Zn. (b) TEM image of $CdSe–Cu_2Se$ NCs obtained by partial CE at room temperature from $Cu_{2-x}Se$ NCs, with elemental mapping of Cu and Cd (c). HRTEM image (d) of a $CdSe–Cu_2Se$ NC with corresponding mean dilation map (e) and fast Fourier transform pattern (f). XRD patterns in (g) display the evolution of the $CdSe–Cu_2Se$ crystal structure with increasing Cd content shown by an arrow. Diagram displaying the evolution of the Cd/Cu ratio in the heavily substoichiometric and close to stoichiometric NCs over the time of the Cu^+-to-Cd^{2+} CE reaction (h). Adapted from ref.[36]. Copyright 2015, American Chemical Society.

Furthermore, we have demonstrated that the pathway of CE reactions can strongly depend on the crystal structure of the host nanoparticles, comparing cubic and hexagonal (metastable) Cu_2Se NCs in Cu-to-Pb exchange performed at room temperature (*Annex 22*).[82] Despite the fact that in both systems the final product of the exchange was rock salt PbSe NCs, in cubic Cu_2Se NCs PbSe nucleated randomly on the overall surface of the host particles, generating Cu_2Se/PbSe core/shell heterostructures as intermediates. This exchange trend, already observed in other CE transformations, can be explained taking into account the low diffusivity of Pb^{2+} ions coupled with the absence of preferred entry points in cubic Cu_2Se. On the other hand, in hexagonal Cu_2Se NCs, Pb^{2+} ions could diffuse and replace host cations along defined (a, b) planes of the host material, generating PbSe stripes sandwiched in between Cu_2Se domains. This peculiar CE process, not observed in any other known system, was attributed to the metastable hexagonal Cu_2Se structure, which offers preferred entry points to the guest ions. Our findings, thus, suggested that the crystal structure of host NCs is an important parameter that should be taken into account when performing CE reactions. More precisely, we observed that both the crystalline quality and morphology of the nanostructures obtained by CE are sensitive to the phase of starting NCs.

2.1.6. Ligand exchange and shell design

Ligand exchange strategy basically consists in replacing ligand molecules, which are inherited in the synthesis, on the surface of NCs, with other ligands that better suit following processing and application of nanoparticles, such as replacement of hydrophobic molecules with hydrophilic ones to impart NCs solubility in aqueous media. This process is particularly important for bio-application of various nanoparticles.[83] For example, by applying mPEG-SH ligand described in *Section 2.1.3*, successful water solubilization of $Cu_{2-x}Te_yS_{1-y}$ NCs with preservation of their plasmonic properties has been realized via the ligand exchange.[32] Another important application of ligand exchange is the synthesis of all-inorganic NCs capped with small charged inorganic species introduced by the Talapin group.[84-87] Such small species drastically improve charge transport in NC-based solids owing to shortening the distance

16

between adjacent particles. Another application of this method is the growth of inorganic shells around semiconductor NCs by alternating anionic and cationic layers, such as S^{2-} and Cd^{2+} to grow CdS at room temperature (*Figure 9a*).[88] We extended this approach to prepare multilayered shells on CdSe NCs made of uniform ZnS and CdS monolayers in several different configurations, as illustrated in *Figure 9b* (*Annex 23*).[44] All core/shell multicomponent nanoparticles preserve narrow size distribution, phase crystallinity, and shape homogeneity of the cores. Combining CdS and ZnS monolayers in various sequences it was possible to finely tune optical properties of the resulting heterostructures. *Figure 9c,d* shows an example of this tuning on CdSe/CdS/ZnS/CdS/ZnS core/multishell QD structure, in which pronounced red shifts in both absorption and PL spectra are observed. Furthermore, using this technique one can alter also the Stokes shift of the QDs (*Figure 9e*). Moreover, we extended the toolbox of the ionic layer deposition to integrate materials with intrinsically different properties, such as Au and CdS in the core/shell structures with substantial lattice mismatch. The results presented in this work demonstrate great opportunities for creating functional materials with programmable properties for electronics and optoelectronics.
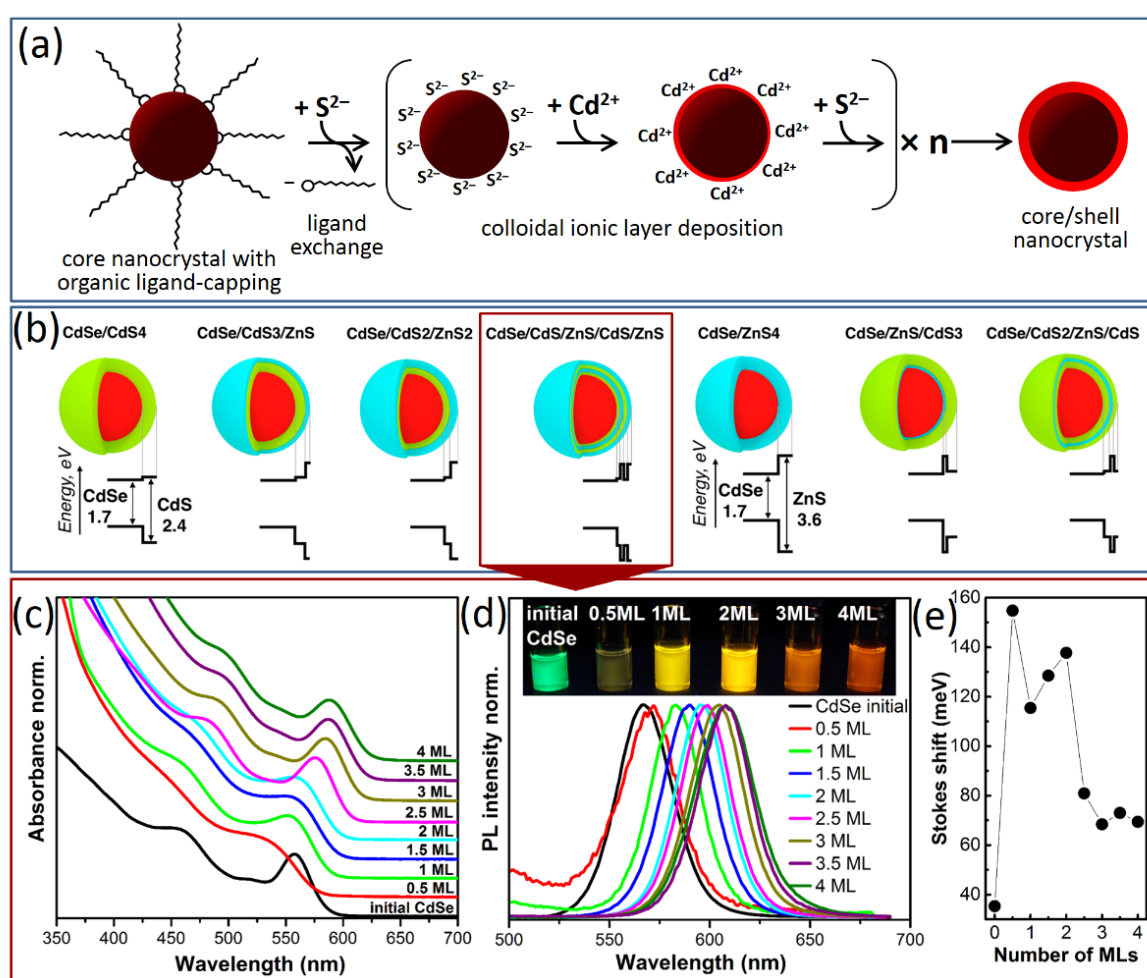

Figure 9. (a) Scheme of the ligand exchange and following ion layer deposition of the CdS shell forming core/shell NCs. (b) Investigated shell combinations with corresponding energy band diagrams of CdSe, CdS, and ZnS. Numbers of layers are indicated after the composition with a final shell thickness of 4 monolayers for all samples. Evolution of the absorption (c) and the PL (b) spectra, as well as values of the Stokes shift (c) of CdSe NCs during their alternate shelling with CdS and ZnS forming the CdSe/CdS/ZnS/CdS/ZnS core/multishell structure. The inset in (d) shows PL color evolution (samples under UV light) during the shell growth. Adapted from ref.[44]. Copyright 2017, American Chemical Society.

2.2. Assembly

Developed assembly approaches relate to non-ordered three dimensional (3D) networking of NCs, also defined as gelation, which yield highly porous structures with large surface area. Three main methods to form these 3D assemblies will be discussed in this section: 1) controllable destabilization of NC colloids, 2) binding through Tz-surface ligands, and 3) electrostatic linking of the all-inorganic NCs via oppositely charged ions.

2.2.1. 3D assembly of thiol-capped nanocrystals via controllable destabilization

Aqueous semiconductor NCs described in **Section 2.1.1** are ideal candidates for further covalent linking and self-assembly such as layer-by-layer deposition mediated by polyelectrolytes, since they are stabilized with short-chain thiols possessing amino-, carboxyl or hydroxyl functional groups.[65, 89] First porous semiconductor metal chalcogenide aerogels made of nanoparticles were reported by the group of Brock.[90-91] Later on, our group introduced a well-controllable and easily up-scalable method to gelate aqueous CdTe QDs via photochemical treatment.[92] The thus produced hydrogels can be further processed by a supercritical drying technique with liquid CO_2. Combination of NCs made of different materials, while capped by similar thiol-containing ligands, in one pot allowed us to produce mixed metal–semiconductor Au–CdTe aerogels (*Annex 24*).[93] We assumed that photochemical treatment induces oxidation of thiolate moieties on the surface of the particles leading to formation of RS–SR bonds thus eventually linking adjacent NCs in one 3D network, as proposed for the formation of the NC gels upon adding an oxidant. The resulting aerogel monoliths consisted of networks of homogeneously dispersed gold and CdTe nanoparticles, which exhibited optical behavior dependent on their composition, while retaining their quantum confinement effects. The variation of the initial CdTe NCs to Au NCs ratio ensured a facile tuning of the content and the properties of the aerogels. Materials of this type combining the optical and catalytic properties of their nano-building blocks with very high porosity of the gel structure are of special interest for applications in sensing and photocatalysis.

Another example of self-assembly of thiol-capped CdTe NCs by means of gentle destabilization is the preparation of 3D CdTe@Cd-TGA hybrid nanostructures, in which large scale nanowires were found as building blocks (*Annex 25*).[94] These structures were formed upon addition of a non-solvent (ethanol) to an aqueous solution of the NCs together with sodium acetate at 70°C. After complete solvent exchange with acetone, these wet 3D hybrid structures were further supercritically dried, yielding solids with a monolith volume of about 1 cm^3 and a density of about 1/2500th of the bulk CdTe. It was found that the nanowires were composed of CdTe@Cd-TGA complex hybrid nanostructures in which well-separated CdTe NCs were uniformly distributed (*Figure 10a*). These nanowires could reach several micrometers in length and approx. 30 nm in width. They maintain quantum confinement of CdTe NCs and thus retain their PL, which may be suitable for the manufacturing of LEDs (e.g., as light-conversion layers), optical sensors, etc.
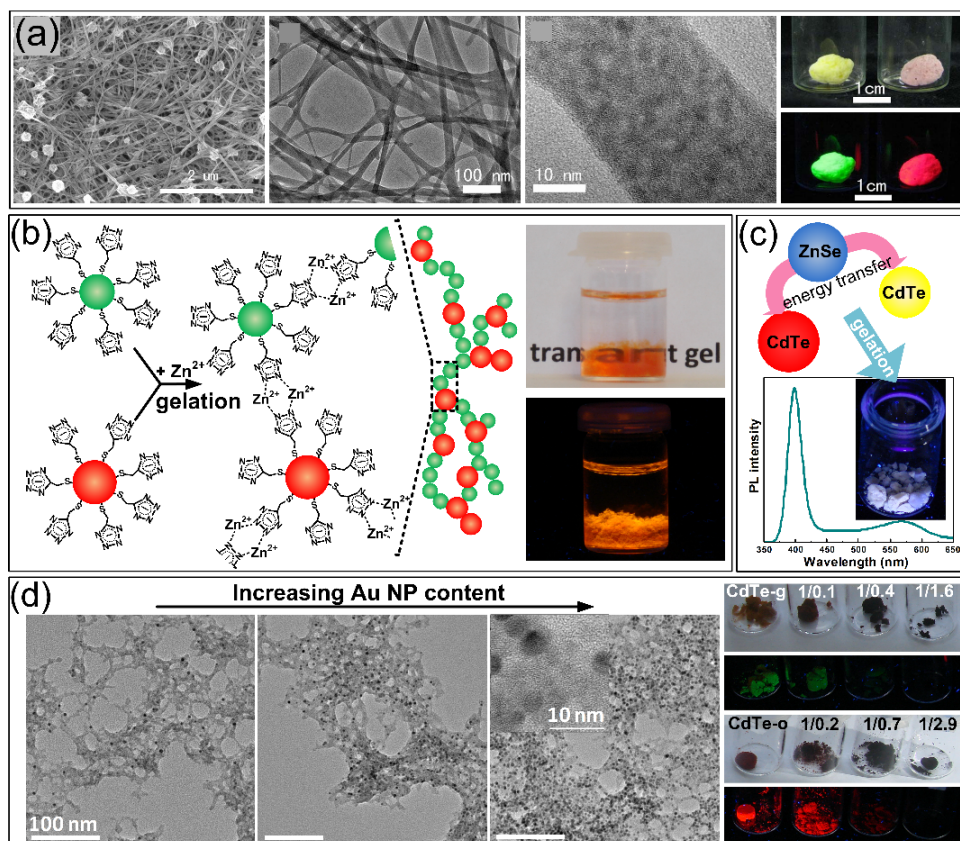
Figure 10. (a) SEM, TEM, and HRTEM images of the 3D CdTe@Cd-TGA complex hybrid nanostructures with photographs of the corresponding dry aerogels under day (top right) and UV (bottom right) light. (b) Scheme of the gelation of two different types of 5-HSCH$_2$Tz-capped NCs by the addition of Zn^{2+} ions (left). Photo of a CdTe NC hydrogel under day (top right) and UV (bottom right) light. (c) Schematics of the preparation of white emitting aerogels by mixing blue-emitting ZnSe, and yellow and red emitting CdTe NCs with their subsequent gelation. PL spectrum and a photograph of the white aerogel under UV light. (d) TEM images of fragments of hybrid CdTe–Au NC aerogels with increasing Au NCs content from left to right. Photos of aerogel samples prepared from green CdTe QDs–Au NCs and orange CdTe QDs–Au NCs mixtures with varied ratios between the particles under day and UV-light (right). Adapted from refs.[40, 94]. Copyright 2010 and 2015, American Chemical Society and Wiley VCH Verlag GmbH & Co.

2.2.2. 3D assembly of tetrazole-capped nanocrystals

Tz-capped CdTe NCs described in **Section 2.1.2** were exploited as building blocks to assemble 3D nanostructures via metal–Tz complexation. Thus, a driving force for the formation of a gel network was a cross-linking of individual NCs by complexation of the tetrazolate units with Zn^{2+} ions, as schematized in *Figure 10b* (*Annex 8*).[37] This approach allows the reproducible and easily upscaleable fabrication of 3D semiconductor networks maintaining the optical properties of the initial NCs. Furthermore, we discovered a unique ability of reversible gelation of these NCs by the competitive complexation of metal ions by a stronger ligand such as ethylenediaminetetraacetic acid. We further elaborated this method to prepare hybrid gels containing semiconductor particles with different band gaps: ZnSe and CdTe, as well as two differently sized fractions of CdTe QDs (*Annex 10*).[39] In these hybrid systems we investigated energy relations between donors and acceptors by means of absorption, steady-state, and time-resolved PL spectroscopy. We found that addition of energy donors compensated the emission quenching of the 3D assembly and resulted in a fine control of its optical properties. The approach ensured a facile preparation of a white-light emitting aerogel via the combination of UV–blue-emitting

ZnSe and yellow- and red-emitting CdTe QDs (*Figure 10c*). These experiments revealed a great potential of the method for the fabrication of LEDs possessing a wide variety of colors. Aerogels can be infiltrated with polymers using a technique recently reported to improve their mechanical properties.[92] Furthermore, they can be hybridized with hole-conducting conjugated polymers to ameliorate the electrical-transport properties of the material.

In addition to mixed semiconductor NC-based (aero)gels, hybrid semiconductor–metal CdTe–Au NCs systems were prepared by the controlled gelation of mixed CdTe and Au NC colloids (*Annex 9*).[38] Simply tuning the initial ratio between CdTe and Au NCs resulted in a precise control of the final aerogel composition owing to the complete cross-linking of all particles present in solution. *Figure 10d* displays TEM images of hybrid CdTe–Au NC aerogels with varying gold content. Apart from Cd^{2+}, other ions like Zn^{2+}, Ba^{2+}, Ni^{2+}, and Ag^+ are applicable for the assembly. The resulting assemblies processed by critical point drying formed highly porous aerogels with the surface area in the range of 50–130 m^2/g and the pore volume of 0.18–0.51 cm^3/g. Optical studies revealed a distinct dependence of the optical properties of the gels on their composition. Gelation and the increase of the gold content in the hybrid architectures induced PL quenching and shortening of the emission lifetime. The method developed is promising for biological and chemical beacon measurements:[95] optical detection of molecules interacting with metal and/or semiconductor nanoparticles in highly porous nanostructures.

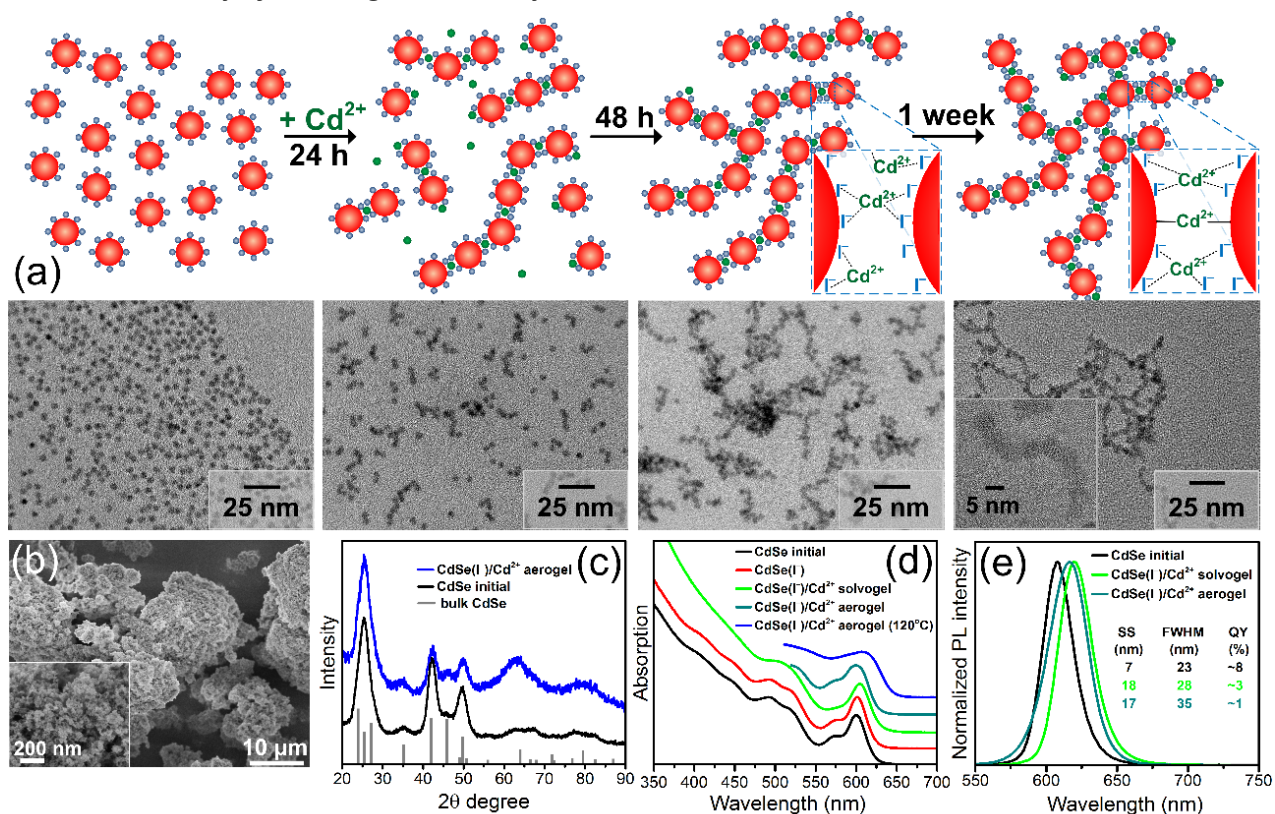### 2.2.3. 3D assembly of all-inorganic nanocrystals

Figure 11. (a) Schematic representation of the gelation process and TEM images showing the gelation of I⁻-capped CdSe NCs in 24 h, 48 h, and one week after the addition of Cd^{2+} linker. (b) SEM image of the corresponding aerogel. (c) XRD patterns of the initial CdSe NCs and the all-inorganic CdSe NC aerogel. (d) Absorption spectra of CdSe NCs before and after the ligand exchange with I⁻, their subsequent gelation with Cd^{2+} in N-methylformamide, and after drying and heat treatment of the resulting aerogel. The spectra are vertically shifted for clarity. (e) PL spectra of the initial CdSe NCs, the CdSe(I⁻)/Cd^{2+} wet gel, and the aerogel,

as well as their corresponding Stokes shifts, FWHM, and PLQY. Adapted from ref.[45]. Copyright 2016, Wiley VCH Verlag GmbH & Co.

All-inorganic semiconductor NCs introduced in **Section 2.1.6** represent another example of suitable building blocks for 3D self-assembly. Therefore, we developed an efficient approach to assemble a variety of electrostatically stabilized all-inorganic NCs by their linking with appropriate ions into multibranched gel networks (*Annex 26*).[45] Among nanomaterials successfully tested in the gel formation were spherical colloidal CdSe, PbS, and PbSe semiconductor NCs with narrow size distributions, as well as CdSe nanoplatelets and ZnO nanorods that were ligand exchanged with different inorganic species, such as S^{2-}, I^-, Cl^-, F^-, as well as Ga/I and In/Cl complexes. The advantage of using charged all-inorganic NCs as building blocks is their inclination to form gel networks through bridging by counterions, as shown in *Figure 11a* on the example of spherical I^--capped CdSe NCs electrostatically linked via Cd^{2+} ions, independent of their size, composition, morphology, and even charge. These all-inorganic nonordered 3D assemblies benefit from strong interparticle coupling, which facilitates charge transport between the NCs. As in the case of the aerogels obtained as described in **Sections 2.2.1** and **2.2.2**, all-inorganic NC assemblies are highly porous monolithic structures (*Figure 11b*), which preserve the quantum confinement of their building blocks (*Figure 11c–e*). For example, the inorganic semiconductor aerogel made of 4.5 nm CdSe NCs capped with I^- ions and bridged with Cd^{2+} ions had a large surface area of up to 150 m^2/g. This approach represents a powerful method to tackle a crucial problem in technological applications of NCs, namely how to build well interconnected all-inorganic 3D structures while retaining the characteristic properties of the individual NCs.

2.3. Applications

Main applications have been accomplished with copper chalcogenide-based nanoparticles, as they are relatively low-toxic and environmentally friendly. Among the materials applied were CIS-based QDs, $Cu_{2-x}Se$ NCs, and CuS superstructures. Thus, CIS-based QDs have been engaged in the fabrication of QDs-in-polymer composites tested as photovoltaic windows, copper selenide nanoparticles were employed to manufacture flexible conductive coatings and as a material with switchable plasmon, copper sulfide hierarchical structures were studied as an electrode material in LIBs.

2.3.1. Copper indium sulfide-based quantum dots-in-polymer composites for luminescent solar concentrators

As has been mentioned above, CIS-based QDs have a great potential for implementation into various devices, in particular those harnessing their excellent optical properties (high extinction coefficient and PLQY values), owing to their low-toxic and environment friendly composition. We exploited this material in luminescent solar concentrator prototypes, schematized in *Figure 12b* (*Annex 27*).[49] This application benefits from the large Stokes shift of CIS-based QDs essential to decrease possible light losses within the device. The QDs embedded into a solid transparent matrix are supposed to absorb energy of the solar light and emit it toward the edges of a plate surrounded by solar cells, thus acting as a light pump.[96] In order to fabricate highly transparent and photostable QDs-in-polymer composites we designed a special surface engineering method, according to which as-synthesized CIS/ZnS or CZIS/ZnS core/shell QDs were first functionalized with 4-vinylaniline and zinc methacrylate, double bond-containing molecules. Then they were processed into bulk composites by free radical

copolymerization with styrene or poly(lauryl methacrylate) in the presence of a common initiator, azobisisobutyronitrile (AIBN) (*Figure 12a, c*).
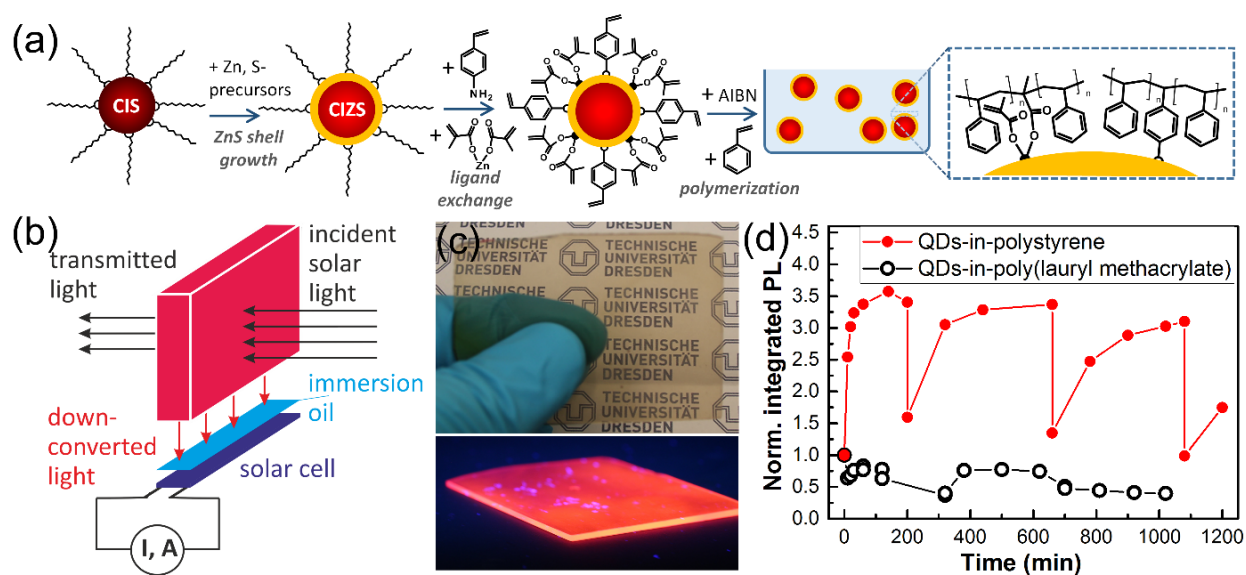

Figure 12. (a) Scheme of the synthesis of the core/shell CZIS/ZnS QDs, ligand exchange with vinylaniline and zinc methacrylate, and free radical copolymerization of these functionalized QDs with styrene into bulk QD-in-polymer composite in the presence of AIBN as an initiator. (b) Scheme of the tested photovoltaic window. (c) Photos of the CZIS/ZnS QD-in-polystyrene composite prepared in the form of a plate under daylight (top) demonstrating its transparency, and under UV excitation (bottom) showing its bright edge. (d) Normalized integrated emission of the QD-in-polymer samples versus time of the illumination. Adapted from ref.[49]. Copyright 2017, Wiley VCH Verlag GmbH & Co.

These QDs-in-polymer composites exhibited high photostability against degradation tested in the focus of a powerful white-light source. Moreover, we observed a particularly interesting light-soaking effect in the case of the QD-in-polystyrene bulk composite that demonstrated at least threefold PL enhancement during the light irradiation (*Figure 12d*). Based on this composite we fabricated solar concentrator prototypes and performed measurements supported by Monte Carlo modeling, which evidenced the stability of samples in conditions of accelerated PL degradation. The developed method of surface engineering can be applied to a wide range of other QDs to incorporate them into a polymer matrix and fabricate highly transparent and stable composites. Our calculations showed that the power produced by a 100×100 mm CIS QDs-based photovoltaic window prototype can reach up to 85–95 mW with an optical performance of 1.1–1.2%, assuming a QY of 50% with 70% average transmittance in the visible region, which can be increased to 175 mW (2.2% optical performance), if the QY can be boosted to 90%.[50] By transferring the transmitted spectrum to the color space, we defined the color of the light behind the window (as delivered to the consumer) and found that QDs with an emission maximum at λ > 795 nm provided inside illumination conditions closest to the white light, with the c-Si solar cell as the optimal choice.

2.3.2. Copper selenide-based conductive flexible coatings

Copper selenide NCs, introduced in **Section 2.1.4**, represent one of the most interesting copper chalcogenide-based materials, since it is a superionic conductor that shows p-type conductivity due to copper vacancies within its crystal lattice.[97-99] Especially promising is the application of these colloidal nanomaterials as conductive coatings in combination with commercially available plastics, since they

can be fabricated via low-cost solution-based techniques, such as drop-casting, spin-coating, spray-deposition, and ink-jet printing. We exploited CuSe NSs (see *Figure 5*) for the fabrication of flexible conductive films prepared by simple drop-casting of the NS dispersions onto polyvinylchloride (PVC), polyvinyl alcohol (PVA), and paper, as shown in *Figure 13a*, without any additional thermal or chemical treatment (*Annex 19*).[46] Further, we studied the electrical properties of these films upon bending, stretching, and folding. The electrical performance of the NSs-based coatings was benchmarked against $Cu_{2-x}Se$ spherical NCs in order to demonstrate the advantage of 2D morphology of the NSs for flexible electronics. The resulting films showed ohmic behavior, with a conductivity of several hundreds of S/m that was maintained for several months under air (*Figure 13b*). The morphology of the NSs-films with overlapping contacts between the individual sheets resulted in an advantageous behavior on flexible substrates, manifested by an almost complete recovery of their conductivity after the application of a mechanical stress such as bending and stretching (*Figure 13c*). At the same time, the similar treatment of $Cu_{2-x}Se$ spherical NCs-based coatings led to irreversible losses of their conductivity that was on the order of 20%–30%. Moreover, the NSs enabled the deposition of conductive films on paper that retained their conductivity under folding, with losses significantly lower than one order of magnitude after several folding cycles. These features make the developed CuSe NSs suitable candidates for printable electronics on flexible substrates (e.g., in medical implantation devices) or for a possible use in stress sensors.
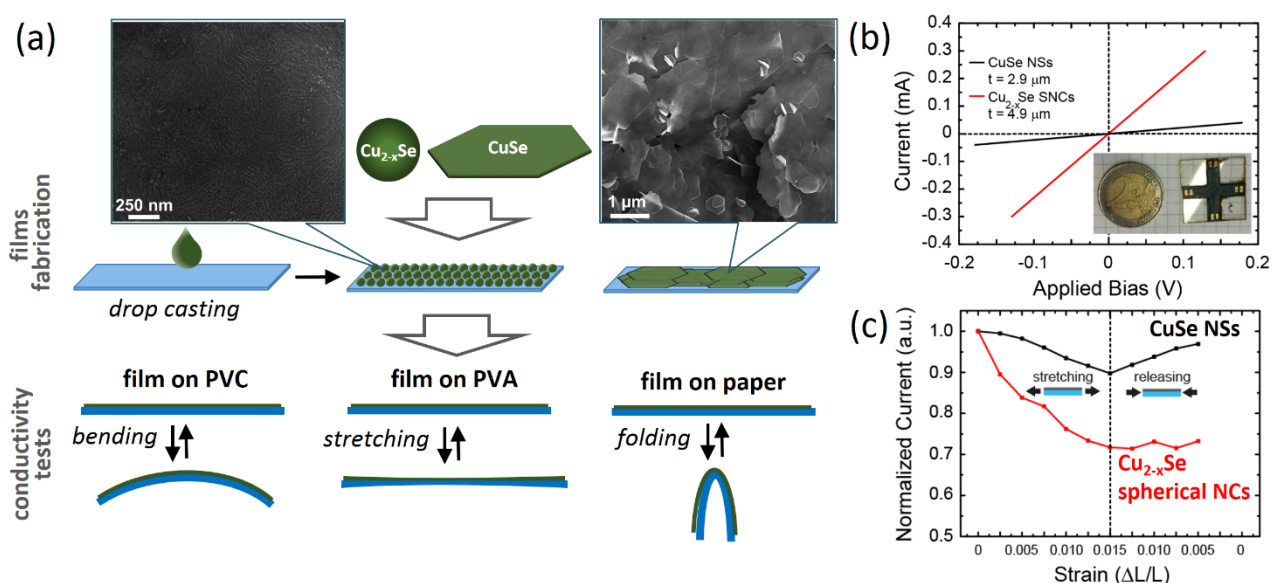

Figure 13. (a) Scheme of the NCs-films preparation from copper selenide spherical particles and NS by drop-casting on various substrates: PVC, PVA, and paper, followed by testing their conductivity upon bending, stretching, and folding, respectively. (b) Typical I–V curve recorded on films of CuSe NSs (average thickness = 2.9 μm) and $Cu_{2-x}Se$ NCs (4.9 μm) on a soda-lime glass. Inset: photo of a typical "Greek cross" sample used for the conductivity measurements, compared in size with a 2€ coin. (c) Performance of stretchable conductive films on PVA fabricated with the both types of nanoparticles. Adapted from ref.[46] Copyright 2016, Wiley VCH Verlag GmbH & Co.

2.3.3. Copper selenide-based electrochromic device

As has been mentioned in **Section 2.1.4** and shown in *Figure 5*, another interesting and important for application property of $Cu_{2-x}Se$ NCs is their strong LSPR in the NIR region stemming from a large number of free holes supported by copper deficient crystal structure of these materials. We introduced an electrochemical method of tuning the LSPR of such degeneratively doped semiconductor NCs by combining cyclic voltammetry and chronoamperometry techniques with absorption spectroscopy

directly *in situ* (*Annex 28*).[48] This approach allowed us to monitor optical changes straightaway during charging/discharging of $Cu_{2-x}Se$ NCs embedded in a transparent ionomer Nafion film deposited onto an indium tin oxide (ITO)-coated glass, as schematized in *Figure 14a*. We observed that LSPR of the $Cu_{2-x}Se$ NCs can be well-controlled and tuned in a wide range simply by potentiostatic switching (*Figure 14b*). Starting with an intensive plasmon of the initial as-synthesized $Cu_{2-x}Se$ NCs we were able to completely damp it via reduction (electron injection). Moreover, this electrochemical tuning was demonstrated to be reversible by subsequent oxidation (extracting electrons from the system). X-ray photoelectron spectroscopy (XPS) analysis of the $Cu_{2-x}Se$ NCs-in-Nafion samples did not reveal any prominent changes in oxidation states of the main elements before and after charging. This allowed us to assign changes in absorption solely to electron injection/extraction processes leading to extinguishing and regenerating free holes present in the as-synthesized NCs. Hence, our findings demonstrated for the first time a reversible tuning of the LSPR of copper chalcogenide NCs without any chemical or structural modification. Such a wide LSPR tunability is of paramount importance, for example in applications of these materials in electrochromic devices to control their transmittance, as well as in photovoltaics to amplify light absorption, and in systems involving plasmon–exciton interactions to controllably quench/enhance light emission.
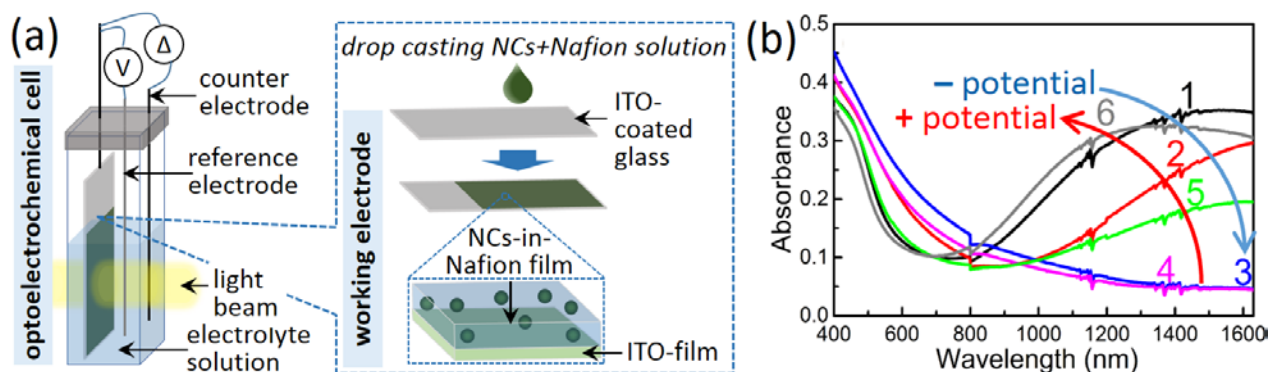

Figure 14. (a) Scheme of the working electrode preparation and electrochemical cell assembly used to measure optical absorption of $Cu_{2-x}Se$ NCs-in-Nafion films in response to electrochemical stimuli *in situ*. (b) Absorption spectra of the $Cu_{2-x}Se$ NCs-in-Nafion film recorded during cyclic voltammetry measurements upon sweeping the potential (charging/discharging of the working electrode). Adapted from ref.[48]. Copyright 2017, American Chemical Society.

2.3.4. Copper sulfide in lithium ion batteries

Copper sulfide micro- and nanostructures, in particular covellite CuS, have attracted considerable interest as electrode materials for LIBs.[100] The main benefits of CuS are its high theoretical capacity, low cost, abundant sources, and low toxicity.[101] In addition, CuS, as a well-known p-type semiconductor, is built up of stacked triangular layers of Cu and S, which makes it especially suitable for LIBs. In LIBs, CuS typically undergoes conversion reactions (e.g., $Cu_xS + 2Li + 2e^- \leftrightarrow Li_2S + xCu$), alloying/dealloying, as well as intercalation/deintercalation (with some reversibility), which lead to sustained capacities in the range of 400–600 mA·h/g.[102] In order to improve properties of this electrode material, in particular its stability in charge/discharge processes, we synthesized CuS superstructures by a facile colloidal approach based on the reaction of copper nitrate with sodium thiosulfate (*Figure 15a*) (*Annex 29*).[47] Depending on the solvent employed (water or a water–ethylene glycol mixture) either ball-like or tubular dandelion-like hierarchical CuS structures were obtained, respectively.
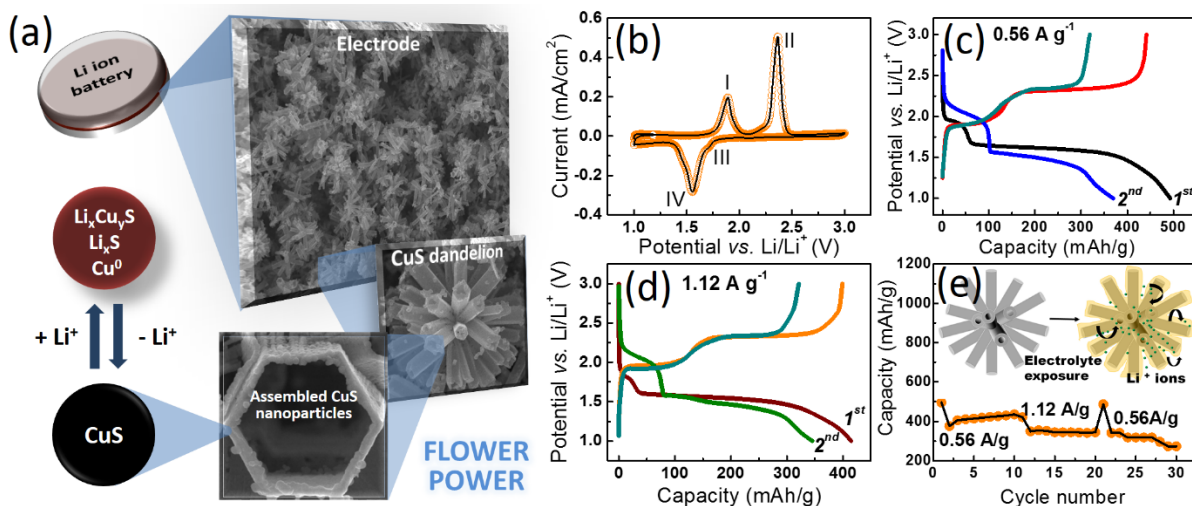
Figure 15. (a) SEM images of the CuS dandelion-like structures and a scheme of the chemical conversion reaction in LIBs. Electrochemical performance of this material: (b) cyclic voltammogram between 1 and 3 V at 0.05 mV/s rate, (c) first two charge/discharge cycles at 0.56 A/g, (d) first two charge/discharge cycles at 1.12 A/g, (e) the cycling characteristics at different current densities. Inset in (e) is a scheme depicting the effective electrolyte immersion that is favorable for a facile Li-ion reaction. Adapted from ref.[47]. Copyright 2015, Wiley VCH Verlag GmbH & Co.

Both of these architectures were assembled of small semispherical 30–40 nm sized nanoparticles, and thus, exhibited similar crystal phases and optical properties. However, these two CuS morphologies were characterized by their markedly different electrochemical performances, suggesting that their complex structures/morphologies influenced the electrochemical properties. From the cyclic voltammetry analysis, we concluded that the particles effectively underwent the redox reactions accounting for conversion processes during charge/discharge (*Figure 15a*). Upon cycling between 1 and 3 V the cells made with CuS dandelion superstructures delivered a good capacity, for example at 0.56 A/g a capacity of approximately 500 mA·h/g was achieved, and the capacity loss after the first cycle was also found to be appreciably low, only by a difference of about 100 mA·h/g (see *Figure 15c*). Similarly, even at high current densities such as 1.12 A/g, the cells exhibited a higher capacity of approximately 425 mA·h/g with a low capacity loss (*Figure 15d,e*). Our electrochemical data indicated that the tubular dandelion-like morphology offered an improved electrochemical performance, over the ball-like assemblies. This particular structure improved both the capacity and the cycling behavior probably due to facile lithiation/delithiation processes on the CuS particles, and also by maximizing the exposure of the particles to the electrolyte (*Figure 15e*). Ease of preparation and processing of these hierarchical nano-microstructures, together with good electrochemical performance, make CuS tubular dandelion-like clusters attractive for developing low-cost LIBs based on conversion reactions.

3. CONCLUSIONS & OUTLOOK

This work summarizes main results accumulated by the author during his work on colloidal semiconductor nanomaterials over last ten years. They embrace a relatively broad field from chemical synthesis of various nanoparticles, through their postsynthetic modification to assembly and application, each supported by a comprehensive characterization. The main compounds studied include II–VI, I–VI, I–III–VI, I–II–III–VI, and I–II–IV–VI semiconductors. In the framework of these investigations facile and easy upscalable aqueous syntheses of alloyed $Zn_xCd_{1-x}Se$, $ZnSe_xTe_{1-x}$, and $Cd_xHg_{1-x}Te$ QDs were

developed. These syntheses produce bright emitting aqueous QDs with extended PL and absorption to the blue and to the NIR region of the spectrum, which widen areas of their potential applications.

Particular focus in the studies was made on copper chalcogenide-based materials, as low-toxic and widely applicable alternatives to more investigated "classical" II–VI systems, such as CdSe. In this direction, by employing the heat-up and the hot-injection approaches binary $Cu_{2-x}S$ and $Cu_{2-x}Se$, as well as quasi-ternary $Cu_{2-x}Se_yS_{1-y}$ and $Cu_{2-x}Te_yS_{1-y}$ NCs were synthesized. Facile shape and crystal structure control was demonstrated on the example of copper selenide nanoparticles allowing for the preparation of monodisperse spherical NCs, nanoplatelets, and large yet thin NSs by means of a simple tuning of basic reaction conditions. Furthermore, these as-prepared binary and quasi-ternary NCs were chemically transformed via CE into more complex alloyed ternary Cu–In–S(Se), quaternary Cu–Zn–In–S(Se), Cu–Zn–Se–S, and quasi-quinary Cu–Zn–Sn–Se–S particles, as well as into Cu_2Se–ZnSe and Cu_2Se–CdSe Janus-like heterostructures. The precise composition control achieved in these nanomaterials was reflected in the fine tuning of their optoelectronic properties. In particular, synthesizing large CISeS/ZnS core/shell QDs we were able to push their fluorescence farther to the NIR, thus significantly extending range of their optical activity. In general, the strategy of partial CE introduced in our work and applied to copper chalcogenide nanoparticles is rather universal and may pave the way to other various complex nanostructures. CuS superstructures were successfully applied as an electrode material in LIBs, based on chemical conversion. Strongly plasmonic self-doped $Cu_{2-x}Se$ NCs were demonstrated as a promising material to be employed in fabrication of electrochromic windows as well as solution-processable conductive coatings. In the latter, CuSe NSs demonstrated their superiority over spherical contenders in the case on flexible substrates.

Special attention in the work was devoted to the surface chemistry of the NCs, since in the case of small nanometer-scaled particles surface plays a crucial role, determining not only their properties but also the ways of further processing and applications. Thus, unique amphiphilic nanoparticles were designed by employing a special short chain PEG molecules functionalized with the thiol group. These NCs were demonstrated to be capable of spontaneous three-phase transfer and of penetration through model and cellular plasma membranes, which makes them a perfect candidate for investigations of inter- and intracellular transport phenomena. Another new ligand successfully employed directly in the synthesis of CdTe and $Zn_xCd_{1-x}Se$ QDs was 5-mercaptomethyltetrazole, which endows the particles with a unique ability to form donor–acceptor complexes with metal cations. Exploiting this property, gels and aerogels assembled from Tz-capped CdTe, CdTe with Au, green CdTe with red CdTe and blue $Zn_xCd_{1-x}Se$ NCs were prepared and studied. Thus, by tuning the ratio between the components in green CdTe–red CdTe–blue $Zn_xCd_{1-x}Se$ QDs aerogel it was possible to fabricate white light emitting assembly of close connected QDs. These porous materials possessing high surface area are perfect candidates for applications in optical sensing, photocatalysis, and lighting.

Another important approach to the surface modification is the ligand exchange to small inorganic species. Based upon this method we developed gelation of all-inorganic capped NCs, bearing a significant surface charge, through the facile electrostatic assembly via oppositely charged ions. For example, CdSe NCs capped with I^- ions were interconnected by adding Cd^{2+} counterions. We demonstrated a general applicability of this gelation approach to a wide range of semiconductor NCs with different morphologies, compositions, and sizes. The resulting 3D structures, as in the case of the gels and aerogels built of Tz-capped NCs, exhibit a large surface area of up to 150 m^2/g. In addition, NC building blocks in these assemblies are not covered by an insulating ligand shell and thus should have better charge transport properties, as compared to as-synthesized organic capped particles, which is

beneficial to application of the obtained (aero)gels in optoelectronics, sensing, catalysis, and thermoelectrics. Furthermore, using the ligand exchange, we developed the precise engineering of the NC shells, in particular CdS, ZnS, and their multilayered combinations, in which CdS and ZnS can be alternated in any sequence. This shell growth was manifested by significant changes in optical properties of the resulting core/shell QDs, especially prominent was the PL shift. A versatility of the shell growth was demonstrated on the synthesis of Au/CdS core/shell NCs, in which a large lattice mismatch between the metal and the semiconductor components makes its direct synthesis based on heterogeneous nucleation very challenging. Special design of the surface of CIS QDs resulted in the fabrication of transparent and photostable QDs-in-polymer composites tested as luminescent solar concentrators. In order to improve compatibility of the QDs with the polymer matrix, they were modified by anchoring copolymerizable molecules.

Overall, despite all progress in the field of colloidal semiconductor NCs achieved up to date, there is still a plenty of room for further fundamental investigations of these unique and versatile materials. In particular, patterns derived by studying "classical systems", such as CdSe and PbS QDs, can be applied to other less developed semiconductor nanoparticles, among which are Cd(Pb, Hg)-free InP- and CIS-based materials, as well as currently booming cesium/alkylammonium lead halide perovskite NCs. Nevertheless, in the author's humble opinion, the chemistry of colloidal NCs has already matured during last decades to the level, where a wide variety of high quality materials can be easily produced by a plethora of synthetic protocols developed to date. Thus, now it is time to turn semiconductor NCs to industrial and commercial lines, not being satisfied with a few successful commercial examples, such as that of Samsung's QLED TVs mentioned in the introduction. One of the hurdles standing on the way of fulfilling expectations of our society in nanomaterials appears to be underdeveloped large-scale production, since most syntheses published to date deal with milligram to gram-scale amounts of precursors and hence resulting products. Large-scale production should go hand in hand with implementation of NC-based optoelectronic devices. In order to advance these two fields, joint contribution of researchers from different specialties, not only chemists and physicists, but also chemical, process, automatization and electrical engineers, programmers (software developers), and managers will be highly required. In this way, development of colloidal nanomaterials will undoubtedly contribute to the general progress of nanotechnology aiming at the level of infiltration into many aspects of life, such as that envisioned in a science fiction novel "The Diamond Age" by Neal Stephenson.

REFERENCES

1.   Alivisatos, A. P., Semiconductor Clusters, Nanocrystals, and Quantum Dots. *Science* **1996**, *271*, 933-937.

2.   Talapin, D. V.; Lee, J.-S.; Kovalenko, M. V.; Shevchenko, E. V., Prospects of Colloidal Nanocrystals for Electronic and Optoelectronic Applications. *Chem. Rev.* **2010**, *110*, 389-458.

3.   Smith, A. M.; Nie, S., Semiconductor Nanocrystals: Structure, Properties, and Band Gap Engineering. *Acc. Chem. Res.* **2010**, *43*, 190-200.

4.   Zherebetskyy, D.; Scheele, M.; Zhang, Y.; Bronstein, N.; Thompson, C.; Britt, D.; Salmeron, M.; Alivisatos, P.; Wang, L.-W., Hydroxylation of the Surface of PbS Nanocrystals Passivated with Oleic Acid. *Science* **2014**, *344*, 1380-1384.

5.   Xia, Y.; Xiong, Y.; Lim, B.; Skrabalak, S. E., Shape-Controlled Synthesis of Metal Nanocrystals: Simple Chemistry Meets Complex Physics? *Angew. Chem. Int. Ed.* **2009**, *48*, 60-103.

6.   Kovalenko, M. V.; Manna, L.; Cabot, A.; Hens, Z.; Talapin, D. V.; Kagan, C. R.; Klimov, V. I.; Rogach, A. L.; Reiss, P.; Milliron, D. J.; Guyot-Sionnnest, P.; Konstantatos, G.; Parak, W. J.; Hyeon, T.; Korgel, B. A.; Murray, C. B.; Heiss, W., Prospects of Nanoscience with Nanocrystals. *ACS Nano* **2015**, *9*, 1012-1057.

7.   Panthani, M. G.; Korgel, B. A., Nanocrystals for Electronics. *Annu. Rev. Chem. Biomol. Eng.* **2012**, *3*, 287-311.

8.   Pelaz, B.; Jaber, S.; de Aberasturi, D. J.; Wulf, V.; Aida, T.; de la Fuente, J. M.; Feldmann, J.; Gaub, H. E.; Josephson, L.; Kagan, C. R.; Kotov, N. A.; Liz-Marzán, L. M.; Mattoussi, H.; Mulvaney, P.; Murray, C. B.; Rogach, A. L.; Weiss, P. S.; Willner, I.; Parak, W. J., The State of Nanoparticle-Based Nanoscience and Biotechnology: Progress, Promises, and Challenges. *ACS Nano* **2012**, *6*, 8468-8483.

9.   Michalet, X.; Pinaud, F. F.; Bentolila, L. A.; Tsay, J. M.; Doose, S.; Li, J. J.; Sundaresan, G.; Wu, A. M.; Gambhir, S. S.; Weiss, S., Quantum Dots for Live Cells, in Vivo Imaging, and Diagnostics. *Science* **2005**, *307*, 538-544.

10.   Sapsford, K. E.; Algar, W. R.; Berti, L.; Gemmill, K. B.; Casey, B. J.; Oh, E.; Stewart, M. H.; Medintz, I. L., Functionalizing Nanoparticles with Biological Molecules: Developing Chemistries That Facilitate Nanotechnology. *Chem. Rev.* **2013**, *113*, 1904-2074.

11.   Medintz, I. L.; Uyeda, H. T.; Goldman, E. R.; Mattoussi, H., Quantum Dot Bioconjugates for Imaging, Labelling and Sensing. *Nat. Mater.* **2005**, *4*, 435-446.

12.   Choi, M. K.; Yang, J.; Kang, K.; Kim, D. C.; Choi, C.; Park, C.; Kim, S. J.; Chae, S. I.; Kim, T.-H.; Kim, J. H.; Hyeon, T.; Kim, D.-H., Wearable Red–Green–Blue Quantum Dot Light-Emitting Diode Array Using High-Resolution Intaglio Transfer Printing. *Nat. Commun.* **2015**, *6*, 7149.

13.   Yang, J.; Choi, M. K.; Kim, D.-H.; Hyeon, T., Designed Assembly and Integration of Colloidal Nanocrystals for Device Applications. *Adv. Mater.* **2016**, *28*, 1176-1207.

14.   Kagan, C. R.; Lifshitz, E.; Sargent, E. H.; Talapin, D. V., Building Devices from Colloidal Quantum Dots. *Science* **2016**, *353*, 885.

15.   Yin, Y.; Alivisatos, A. P., Colloidal Nanocrystal Synthesis and the Organic-Inorganic Interface. *Nature* **2005**, *437*, 664-670.

16.   Schmid, G., *Nanoparticles: From Theory to Application*. 2nd ed.; WILEY-VCH Verlag GmbH & Co. KGaA: Weinheim, 2010; p 533.

17.   Klimov, V. I., *Semiconductor and Metal Nanocrystals: Synthesis and Electronic and Optical Properties*. 1st ed.; Marcel Dekker, Inc.: New York, 2004; p 500.

18.   Rogach, A. L., *Semiconductor Nanocrystal Quantum Dots: Synthesis, Assembly, Spectroscopy and Applications*. Springer-Verlag: Wien, 2008; p 372.

19.   Lee, J.; Yang, J.; Kwon, S. G.; Hyeon, T., Nonclassical Nucleation and Growth of Inorganic Nanoparticles. *Nat. Rev. Mater.* **2016**, *1*, 16034.

20.   Kwon, S. G.; Piao, Y.; Park, J.; Angappane, S.; Jo, Y.; Hwang, N.-M.; Park, J.-G.; Hyeon, T., Kinetics of Monodisperse Iron Oxide Nanocrystal Formation by "Heating-up" Process. *J. Am. Chem. Soc.* **2007**, *129*, 12571-12584.

21.   Kim, B. H.; Shin, K.; Kwon, S. G.; Jang, Y.; Lee, H.-S.; Lee, H.; Jun, S. W.; Lee, J.; Han, S. Y.; Yim, Y.-H.; Kim, D.-H.; Hyeon, T., Sizing by Weighing: Characterizing Sizes of Ultrasmall-Sized Iron Oxide Nanocrystals Using MALDI-TOF Mass Spectrometry. *J. Am. Chem. Soc.* **2013**, *135*, 2407-2410.

22.   Yang, J.; Fainblat, R.; Kwon, S. G.; Muckel, F.; Yu, J. H.; Terlinden, H.; Kim, B. H.; Iavarone, D.; Choi, M. K.; Kim, I. Y.; Park, I.; Hong, H.-K.; Lee, J.; Son, J. S.; Lee, Z.; Kang, K.; Hwang, S.-J.; Bacher, G.; Hyeon, T., Route to the Smallest Doped Semiconductor: Mn^{2+}-Doped $(CdSe)_{13}$ Clusters. *J. Am. Chem. Soc.* **2015**, *137*, 12776-12779.

23.   Murray, C. B.; Norris, D. J.; Bawendi, M. G., Synthesis and Characterization of Nearly Monodisperse CdE (E = Sulfur, Selenium, Tellurium) Semiconductor Nanocrystallites. *J. Am. Chem. Soc.* **1993**, *115*, 8706-15.

24.   Park, J.; Joo, J.; Soon, G. K.; Jang, Y.; Hyeon, T., Synthesis of Monodisperse Spherical Nanocrystals. *Angew. Chem. Int. Ed.* **2007**, *46*, 4630-4660.

25.   Thanh, N. T. K.; Maclean, N.; Mahiddine, S., Mechanisms of Nucleation and Growth of Nanoparticles in Solution. *Chem. Rev.* **2014**, *114*, 7610-7630.

26.   LaMer, V. K.; Dinegar, R. H., Theory, Production and Mechanism of Formation of Monodispersed Hydrosols. *J. Am. Chem. Soc.* **1950**, *72*, 4847-4854.

27.   Lesnyak, V.; Plotnikov, A.; Gaponik, N.; Eychmüller, A., Toward Efficient Blue-Emitting Thiol-Capped $Zn_{1-x}Cd_xSe$ Nanocrystals. *J. Mater. Chem.* **2008**, *18*, 5142-5146.

28.   Lesnyak, V.; Dubavik, A.; Plotnikov, A.; Gaponik, N.; Eychmüller, A., One-Step Aqueous Synthesis of Blue-Emitting Glutathione-Capped $ZnSe_{1-x}Te_x$ Alloyed Nanocrystals. *Chem. Commun.* **2010**, *46*, 886-888.

29.   Lesnyak, V.; Lutich, A.; Gaponik, N.; Grabolle, M.; Plotnikov, A.; Resch-Genger, U.; Eychmüller, A., One-Pot Aqueous Synthesis of High Quality Near Infrared Emitting $Cd_{1-x}Hg_xTe$ Nanocrystals. *J. Mater. Chem.* **2009**, *19*, 9147-9152.

30.   Raevskaya, A.; Lesnyak, V.; Haubold, D.; Dzhagan, V.; Stroyuk, O.; Gaponik, N.; Zahn, D. R. T.; Eychmüller, A., A Fine Size Selection of Brightly Luminescent Water-Soluble Ag–In–S and Ag–In–S/ZnS Quantum Dots. *J. Phys. Chem. C* **2017**, *121*, 9032-9042.

31.   Lesnyak, V.; Gaponik, N.; Eychmüller, A., Colloidal Semiconductor Nanocrystals: The Aqueous Approach. *Chem. Soc. Rev.* **2013**, *42*, 2905-2929.

32.   Saldanha, P. L.; Brescia, R.; Prato, M.; Li, H.; Povia, M.; Manna, L.; Lesnyak, V., Generalized One-Pot Synthesis of Copper Sulfide, Selenide-Sulfide, and Telluride-Sulfide Nanoparticles. *Chem. Mater.* **2014**, *26*, 1442-1449.

33.   Akkerman, Q. A.; Genovese, A.; George, C.; Prato, M.; Moreels, I.; Casu, A.; Marras, S.; Curcio, A.; Scarpellini, A.; Pellegrino, T.; Manna, L.; Lesnyak, V., From Binary Cu_2S to Ternary Cu–In–S and Quaternary Cu–In–Zn–S Nanocrystals with Tunable Composition via Partial Cation Exchange. *ACS Nano* **2015**, *9*, 521-531.

34.   Lox, J. F. L.; Dang, Z.; Dzhagan, V. M.; Spittel, D.; Martín-García, B.; Moreels, I.; Zahn, D. R. T.; Lesnyak, V., Near-Infrared Cu–In–Se-Based Colloidal Nanocrystals via Cation Exchange. *Chem. Mater.* **2018**, *30*, 2607-2617.

35.   Lesnyak, V.; George, C.; Genovese, A.; Prato, M.; Casu, A.; Ayyappan, S.; Scarpellini, A.; Manna, L., Alloyed Copper Chalcogenide Nanoplatelets via Partial Cation Exchange Reactions. *ACS Nano* **2014**, *8*, 8407-8418.

36.   Lesnyak, V.; Brescia, R.; Messina, G. C.; Manna, L., Cu Vacancies Boost Cation Exchange Reactions in Copper Selenide Nanocrystals. *J. Am. Chem. Soc.* **2015**, *137*, 9315-9323.

37.   Lesnyak, V.; Voitekhovich, S. V.; Gaponik, P. N.; Gaponik, N.; Eychmüller, A., CdTe Nanocrystals Capped with a Tetrazolyl Analogue of Thioglycolic Acid: Aqueous Synthesis, Characterization, and Metal-Assisted Assembly. *ACS Nano* **2010**, *4*, 4090-4096.

38.   Lesnyak, V.; Wolf, A.; Dubavik, A.; Borchardt, L.; Voitekhovich, S. V.; Gaponik, N.; Kaskel, S.; Eychmüller, A., 3D Assembly of Semiconductor and Metal Nanocrystals: Hybrid CdTe/Au Structures with Controlled Content. *J. Am. Chem. Soc.* **2011**, *133*, 13413-13420.

39.   Wolf, A.; Lesnyak, V.; Gaponik, N.; Eychmüller, A., Quantum-Dot-Based (Aero)Gels: Control of the Optical Properties. *J. Phys. Chem. Lett.* **2012**, *3*, 2188-2193.

40.   Voitekhovich, S. V.; Lesnyak, V.; Gaponik, N.; Eychmüller, A., Tetrazoles: Unique Capping Ligands and Precursors for Nanostructured Materials. *Small* **2015**, *11*, 5728-5739.

41.   Dubavik, A.; Lesnyak, V.; Gaponik, N.; Eychmüller, A., One-Phase Synthesis of Gold Nanoparticles with Varied Solubility. *Langmuir* **2011**, *27*, 10224-10227.

42.   Dubavik, A.; Lesnyak, V.; Thiessen, W.; Gaponik, N.; Wolff, T.; Eychmüller, A., Synthesis of Amphiphilic CdTe Nanocrystals. *J. Phys. Chem. C* **2009**, *113*, 4748-4750.

43.   Dubavik, A.; Sezgin, E.; Lesnyak, V.; Gaponik, N.; Schwille, P.; Eychmüller, A., Penetration of Amphiphilic Quantum Dots through Model and Cellular Plasma Membranes. *ACS Nano* **2012**, *6*, 2150-2156.

44.   Slejko, E. A.; Sayevich, V.; Cai, B.; Gaponik, N.; Lughi, V.; Lesnyak, V.; Eychmüller, A., Precise Engineering of Nanocrystal Shells via Colloidal Atomic Layer Deposition. *Chem. Mater.* **2017**, *29*, 8111-8118.

45.   Sayevich, V.; Cai, B.; Benad, A.; Haubold, D.; Sonntag, L.; Gaponik, N.; Lesnyak, V.; Eychmüller, A., 3D Assembly of All-Inorganic Colloidal Nanocrystals into Gels and Aerogels. *Angew. Chem. Int. Ed.* **2016**, *55*, 6334-6338.

46.   Vikulov, S.; Di Stasio, F.; Ceseracciu, L.; Saldanha, P. L.; Scarpellini, A.; Dang, Z.; Krahne, R.; Manna, L.; Lesnyak, V., Fully Solution-Processed Conductive Films Based on Colloidal Copper Selenide Nanosheets for Flexible Electronics. *Adv. Funct. Mater.* **2016**, *26*, 3670-3677.

47.   Hosseinpour, Z.; Scarpellini, A.; Najafishirtari, S.; Marras, S.; Colombo, M.; Alemi, A.; Volder, M. D.; George, C.; Lesnyak, V., Morphology-Dependent Electrochemical Properties of CuS Hierarchical Superstructures. *ChemPhysChem* **2015**, *16*, 3418-3424.

48.   Llorente, V. B.; Dzhagan, V. M.; Gaponik, N.; Iglesias, R. A.; Zahn, D. R. T.; Lesnyak, V., Electrochemical Tuning of Localized Surface Plasmon Resonance in Copper Chalcogenide Nanocrystals. *J. Phys. Chem. C* **2017**, *121*, 18244-18253.

49.   Lesyuk, R.; Cai, B.; Reuter, U.; Gaponik, N.; Popovych, D.; Lesnyak, V., Quantum-Dot-in-Polymer Composites via Advanced Surface Engineering. *Small Methods* **2017**, *1*, 1700189.

50.   Lesyuk, R.; Lesnyak, V.; Herguth, A.; Popovych, D.; Bobitski, Y.; Klinke, C.; Gaponik, N., Simulation Study of Environmentally Friendly Quantum-Dot-Based Photovoltaic Windows. *J. Mater. Chem. C* **2017**, *5*, 11790-11797.

51.   Weller, H., Colloidal Semiconductor Q-Particles: Chemistry in the Transition Region between Solid State and Molecules. *Angew. Chem. Int. Ed.* **1993**, *32*, 41-53.

52.   Henglein, A., Small-Particle Research – Physicochemical Properties of Extremely Small Colloidal Metal and Semiconductor Particles. *Chem. Rev.* **1989**, *89*, 1861-1873.

53.   Rogach, A. L.; Franzl, T.; Klar, T. A.; Feldmann, J.; Gaponik, N.; Lesnyak, V.; Shavel, A.; Eychmüller, A.; Rakovich, Y. P.; Donegan, J. F., Aqueous Synthesis of Thiol-Capped CdTe Nanocrystals: State-of-the-Art. *J. Phys. Chem. C* **2007**, *111*, 14628-14637.

54.   Li, Y.; Jing, L.; Qiao, R.; Gao, M., Aqueous Synthesis of CdTe Nanocrystals: Progresses and Perspectives. *Chem. Commun.* **2011**, *47*, 9293-9311.

55.   Jing, L.; Kershaw, S. V.; Li, Y.; Huang, X.; Li, Y.; Rogach, A. L.; Gao, M., Aqueous Based Semiconductor Nanocrystals. *Chem. Rev.* **2016**, *116*, 10623-10730.

56.   Lesnyak, V.; Gaponik, N.; Eychmüller, A., Aqueous Synthesis of Colloidal CdTe Nanocrystals. In *Cadmium Telluride Quantum Dots: Advances and Applications*, Donegan, J.; Rakovich, Y., Eds. Pan Stanford Publishing Pte. Ltd.: Singapore, 2013; pp 23-60.

57.   Regulacio, M. D.; Han, M.-Y., Composition-Tunable Alloyed Semiconductor Nanocrystals. *Acc. Chem. Res.* **2010**, *43*, 621-630.

58.   Rajh, T.; Micic, O. I.; Nozik, A. J., Synthesis and Characterization of Surface-Modified Colloidal Cadmium Telluride Quantum Dots. *J. Phys. Chem.* **1993**, *97*, 11999-2003.

59.   Ingole, P. P.; Lesnyak, V.; Tatikondewar, L.; Leubner, S.; Gaponik, N.; Kshirsagar, A.; Eychmüller, A., Probing Absolute Electronic Energy Levels in Hg-Doped CdTe Semiconductor Nanocrystals by Electrochemistry and Density Functional Theory. *ChemPhysChem* **2016**, *17*, 244-252.

60.   Osipovich, N. P.; Poznyak, S. K.; Lesnyak, V.; Gaponik, N., Cyclic Voltammetry as a Sensitive Method for in Situ Probing of Chemical Transformations in Quantum Dots. *Phys. Chem. Chem. Phys.* **2016**, *18*, 10355-10361.

61.   Aldakov, D.; Lefrancois, A.; Reiss, P., Ternary and Quaternary Metal Chalcogenide Nanocrystals: Synthesis, Properties and Applications. *J. Mater. Chem. C* **2013**, *1*, 3756-3776.

62.   Coughlan, C.; Ibáñez, M.; Dobrozhan, O.; Singh, A.; Cabot, A.; Ryan, K. M., Compound Copper Chalcogenide Nanocrystals. *Chem. Rev.* **2017**, *117*, 5865-6109.

63.   Kolny-Olesiak, J.; Weller, H., Synthesis and Application of Colloidal $CuInS_2$ Semiconductor Nanocrystals. *ACS Appl. Mater. Interfaces* **2013**, *5*, 12221-12237.

64.   Stroyuk, O.; Raevskaya, A.; Gaponik, N., Solar Light Harvesting with Multinary Metal Chalcogenide Nanocrystals. *Chem. Soc. Rev.* **2018**, *47*, 5354-5422.

65.   Gaponik, N., Assemblies of Thiol-Capped Nanocrystals as Building Blocks for Use in Nanotechnology. *J. Mater. Chem.* **2010**, *20*, 5174-5181.

66.   Gaponik, N.; Rogach, A. L., Thiol-Capped CdTe Nanocrystals: Progress and Perspectives of the Related Research Fields. *Phys. Chem. Chem. Phys.* **2010**, *12*, 8685-8693.

67.   Dubavik, A.; Lesnyak, V.; Gaponik, N.; Eychmüller, A., A Versatile Approach for a Variety of Amphiphilic Nanoparticles: Semiconductor – Plasmonic – Magnetic. *Z. Phys. Chem.* **2014**, *228*, 171-181.

68.   van der Stam, W.; Gudjonsdottir, S.; Evers, W. H.; Houtepen, A. J., Switching between Plasmonic and Fluorescent Copper Sulfide Nanocrystals. *J. Am. Chem. Soc.* **2017**, *139*, 13208-13217.

69.   Comin, A.; Manna, L., New Materials for Tunable Plasmonic Colloidal Nanocrystals. *Chem. Soc. Rev.* **2014**, *43*, 3957-3975.

70.   Mattox, T. M.; Ye, X.; Manthiram, K.; Schuck, P. J.; Alivisatos, A. P.; Urban, J. J., Chemical Control of Plasmons in Metal Chalcogenide and Metal Oxide Nanostructures. *Adv. Mater.* **2015**, *27*, 5830-5837.

71.   Liu, X.; Swihart, M. T., Heavily-Doped Colloidal Semiconductor and Metal Oxide Nanocrystals: An Emerging New Class of Plasmonic Nanomaterials. *Chem. Soc. Rev.* **2014**, *43*, 3908-3920.

72.   Faucheaux, J. A.; Stanton, A. L. D.; Jain, P. K., Plasmon Resonances of Semiconductor Nanocrystals: Physical Principles and New Opportunities. *J. Phys. Chem. Lett.* **2014**, *5*, 976-985.

73.   Zhao, Y.; Burda, C., Development of Plasmonic Semiconductor Nanomaterials with Copper Chalcogenides for a Future with Sustainable Energy Materials. *Energy Environ. Sci.* **2012**, *5*, 5564-5576.

74.   Kriegel, I.; Scotognella, F.; Manna, L., Plasmonic Doped Semiconductor Nanocrystals: Properties, Fabrication, Applications and Perspectives. *Phys. Rep.* **2017**, *674*, 1-52.

75.   Agrawal, A.; Cho, S. H.; Zandi, O.; Ghosh, S.; Johns, R. W.; Milliron, D. J., Localized Surface Plasmon Resonance in Semiconductor Nanocrystals. *Chem. Rev.* **2018**, *118*, 3121-3207.

76.   Saldanha, P. L.; Lesnyak, V.; Manna, L., Large Scale Syntheses of Colloidal Nanomaterials. *Nano Today* **2017**, *12*, 46-63.

77.   De Trizio, L.; Manna, L., Forging Colloidal Nanostructures via Cation Exchange Reactions. *Chem. Rev.* **2016**, *116*, 10852-10887.

78.   Beberwyck, B. J.; Surendranath, Y.; Alivisatos, A. P., Cation Exchange: A Versatile Tool for Nanomaterials Synthesis. *J. Phys. Chem. C* **2013**, *117*, 19759-19770.

79.   Gupta, S.; Kershaw, S. V.; Rogach, A. L., 25th Anniversary Article: Ion Exchange in Colloidal Nanocrystals. *Adv. Mater.* **2013**, *25*, 6923-6944.

80.   Rivest, J. B.; Jain, P. K., Cation Exchange on the Nanoscale: An Emerging Technique for New Material Synthesis, Device Fabrication, and Chemical Sensing. *Chem. Soc. Rev.* **2013**, *42*, 89-96.

81.   Moon, G. D.; Ko, S.; Min, Y.; Zeng, J.; Xia, Y.; Jeong, U., Chemical Transformations of Nanostructured Materials. *Nano Today* **2011**, *6*, 186-203.

82.   Gariano, G.; Lesnyak, V.; Brescia, R.; Bertoni, G.; Dang, Z.; Gaspari, R.; De Trizio, L.; Manna, L., Role of the Crystal Structure in Cation Exchange Reactions Involving Colloidal Cu_2Se Nanocrystals. *J. Am. Chem. Soc.* **2017**, *139*, 9583-9590.

83.   Sperling, R. A.; Parak, W. J., Surface Modification, Functionalization and Bioconjugation of Colloidal Inorganic Nanoparticles. *Phil. Trans. R. Soc. A* **2010**, *368*, 1333-1383.

84.   Kovalenko, M. V.; Scheele, M.; Talapin, D. V., Colloidal Nanocrystals with Molecular Metal Chalcogenide Surface Ligands. *Science* **2009**, *324*, 1417-1420.

85.   Kovalenko, M. V.; Bodnarchuk, M. I.; Zaumseil, J.; Lee, J. S.; Talapin, D. V., Expanding the Chemical Versatility of Colloidal Nanocrystals Capped with Molecular Metal Chalcogenide Ligands. *J. Am. Chem. Soc.* **2010**, *132*, 10085-10092.

86.   Nag, A.; Kovalenko, M. V.; Lee, J.-S.; Liu, W.; Spokoyny, B.; Talapin, D. V., Metal-Free Inorganic Ligands for Colloidal Nanocrystals: S^{2-}, HS^-, Se^{2-}, HSe^-, Te^{2-}, HTe^-, TeS_3^{2-}, OH^-, and NH_2^- as Surface Ligands. *J. Am. Chem. Soc.* **2011**, *133*, 10612-10620.

87.   Boles, M. A.; Ling, D.; Hyeon, T.; Talapin, D. V., The Surface Science of Nanocrystals. *Nat. Mater.* **2016**, *15*, 141-153.

88.   Ithurria, S.; Talapin, D. V., Colloidal Atomic Layer Deposition (c-ALD) Using Self-Limiting Reactions at Nanocrystal Surface Coupled to Phase Transfer between Polar and Nonpolar Media. *J. Am. Chem. Soc.* **2012**, *134*, 18585-18590.

89.   Lesnyak, V.; Gaponik, N., Aqueous Based Colloidal Quantum Dots for Optoelectronics. In *Colloidal Quantum Dot Optoelectronics and Photovoltaics*, Konstantatos, G.; Sargent, E. H., Eds. Cambridge University Press: New York, 2013; pp 30-58.

90.   Mohanan, J. L.; Arachchige, I. U.; Brock, S. L., Porous Semiconductor Chalcogenide Aerogels. *Science* **2005**, *307*, 397-400.

91.   Arachchige, I. U.; Brock, S. L., Sol-Gel Methods for the Assembly of Metal Chalcogenide Quantum Dots. *Acc. Chem. Res.* **2007**, *40*, 801-809.

92.   Gaponik, N.; Wolf, A.; Marx, R.; Lesnyak, V.; Schilling, K.; Eychmüller, A., Three-Dimensional Self-Assembly of Thiol-Capped CdTe Nanocrystals: Gels and Aerogels as Building Blocks for Nanotechnology. *Adv. Mater.* **2008**, *20*, 4257-4262.

93.   Hendel, T.; Lesnyak, V.; Kühn, L.; Herrmann, A.-K.; Bigall, N. C.; Borchardt, L.; Kaskel, S.; Gaponik, N.; Eychmüller, A., Mixed Aerogels from Au and CdTe Nanoparticles. *Adv. Funct. Mater.* **2013**, *23*, 1903-1911.

94.   Chen, H.; Lesnyak, V.; Bigall, N. C.; Gaponik, N.; Eychmüller, A., Self-Assembly of TGA-Capped CdTe Nanocrystals into Three-Dimensional Luminescent Nanostructures. *Chem. Mater.* **2010**, *22*, 2309-2314.

95.   Suzuki, Y.; Yokoyama, K., Development of Functional Fluorescent Molecular Probes for the Detection of Biological Substances. *Biosensors* **2015**, *5*, 337.

96.   Zhou, Y.; Zhao, H.; Ma, D.; Rosei, F., Harnessing the Properties of Colloidal Quantum Dots in Luminescent Solar Concentrators. *Chem. Soc. Rev.* **2018**, *47*, 5866-5890.

97.   Riha, S. C.; Johnson, D. C.; Prieto, A. L., Cu_2Se Nanoparticles with Tunable Electronic Properties Due to a Controlled Solid-State Phase Transition Driven by Copper Oxidation and Cationic Conduction. *J. Am. Chem. Soc.* **2011**, *133*, 1383-1390.

98.   Deka, S.; Genovese, A.; Zhang, Y.; Miszta, K.; Bertoni, G.; Krahne, R.; Giannini, C.; Manna, L., Phosphine-Free Synthesis of p-Type Copper(I) Selenide Nanocrystals in Hot Coordinating Solvents. *J. Am. Chem. Soc.* **2010**, *132*, 8912-8914.

99.   Liu, Y.-Q.; Wang, F.-X.; Xiao, Y.; Peng, H.-D.; Zhong, H.-J.; Liu, Z.-H.; Pan, G.-B., Facile Microwave-Assisted Synthesis of Klockmannite CuSe Nanosheets and Their Exceptional Electrical Properties. *Sci. Rep.* **2014**, *4*, 5998.

100.   Zhang, Q.; Uchaker, E.; Candelaria, S. L.; Cao, G., Nanomaterials for Energy Conversion and Storage. *Chem. Soc. Rev.* **2013**, *42*, 3127-3171.

101.   Gao, M.-R.; Xu, Y.-F.; Jiang, J.; Yu, S.-H., Nanostructured Metal Chalcogenides: Synthesis, Modification, and Applications in Energy Conversion and Storage Devices. *Chem. Soc. Rev.* **2013**, *42*, 2986-3017.

102.   Débart, A.; Dupont, L.; Patrice, R.; Tarascon, J. M., Reactivity of Transition Metal (Co, Ni, Cu) Sulphides Versus Lithium: The Intriguing Case of the Copper Sulphide. *Solid State Sci.* **2006**, *8*, 640-651.

ACKNOWLEDGEMENTS

I am grateful to my *Alma Mater*, the Belarussian State University, for being a grate school. I am very much in debt to Dr. Ludmila V. Gaponik and Prof. Pavel N. Gaponik who took me in the wonderful world of science being my teachers, mentors, and second parents.

Last, but certainly not least, I express my deepest gratitude to my family, and especially to my wife Lena for her love, patience, understanding, belief, and continuous support.

List of annexes including a statement of the author's own contribution to jointly published papers

Annex 1.
Lesnyak V., Plotnikov A., Gaponik N., Eychmüller A.
Toward efficient blue-emitting thiol-capped $Zn_{1-x}Cd_xSe$ nanocrystals.
J. Mater. Chem., **2008**, *18*, 5142–5146.
https://pubs.rsc.org/en/content/articlelanding/2008/jm/b811859k#!divAbstract
I performed the majority of experiments on the synthesis and characterization of the NCs. I wrote the manuscript draft and I am the corresponding author.

Annex 2.
Lesnyak V., Dubavik A., Plotnikov A., Gaponik N., Eychmüller A.
One-step aqueous synthesis of blue-emitting glutathione-capped $ZnSe_{1-x}Te_x$ alloyed nanocrystals.
Chem. Commun., **2010**, *46*, 886–888.
https://pubs.rsc.org/en/content/articlelanding/2010/cc/b919986a#!divAbstract
I performed the majority of experiments on the synthesis and characterization of the NCs. I wrote the manuscript draft and I am the corresponding author.

Annex 3.
Lesnyak V., Lutich A., Gaponik N., Grabolle M., Plotnikov A., Resch-Genger U., Eychmüller A.
One-pot aqueous synthesis of high quality near infrared emitting $Cd_{1-x}Hg_xTe$ nanocrystals.
J. Mater. Chem., **2009**, *19*, 9147–9152.
https://pubs.rsc.org/en/content/articlelanding/2009/jm/b913200g#!divAbstract
I performed the majority of experiments on the synthesis and characterization of the NCs. I wrote the manuscript draft.

Annex 4.
Ingole P. P., Lesnyak V., Tatikondewar L., Leubner S., Gaponik N., Kshirsagar A., Eychmüller A.
Probing absolute electronic energy levels in Hg-doped CdTe semiconductor nanocrystals by electrochemistry and density functional theory.
ChemPhysChem, **2016**, *17*, 244–252.
https://chemistry-europe.onlinelibrary.wiley.com/doi/full/10.1002/cphc.201501026
I performed the synthesis of the materials, their optical characterization and contributed to discussions and writing.

Annex 5.
Osipovich N., Poznyak S. K., Lesnyak V., Gaponik N.
Cyclic voltammetry as a sensitive method for in-situ probing of chemical transformations in quantum dots.
Phys. Chem. Chem. Phys., **2016**, *18*, 10355–10361.
https://pubs.rsc.org/en/content/articlelanding/2016/cp/c6cp01085g#!divAbstract
I synthesized the materials, performed their optical characterization. I also coordinated preparation of the manuscript contributing to discussions and writing. I am one of the two corresponding authors.

Annex 6.
Raevskaya A., Lesnyak V., Haubold D., Dzhagan V., Stroyuk O., Gaponik N., Zahn D. R. T., Eychmüller A.
A fine size selection of brightly luminescent water-soluble Ag–In–S and Ag–In–S/ZnS quantum dots.
J. Phys. Chem. C **2017**, *121*, 9032–9042.
https://pubs.acs.org/doi/10.1021/acs.jpcc.7b00849
I initiated this work and contributed to the experiments, discussions and writing.

Annex 7.

Lesnyak V., Gaponik N., Eychmüller A.

Colloidal semiconductor nanocrystals: the aqueous approach.

Chem. Soc. Rev., **2013**, *42*, 2905–2929.

https://pubs.rsc.org/en/content/articlelanding/2013/cs/c2cs35285k#!divAbstract

I wrote the draft of the manuscript.

Annex 8.

Lesnyak V., Voitekhovich S. V., Gaponik P. N., Gaponik N., Eychmüller A.

CdTe nanocrystals capped with a tetrazolyl analogue of thioglycolic acid: aqueous synthesis, characterization, and metal-assisted assembly.

ACS Nano, **2010**, *4*, 4090–4096.

https://pubs.acs.org/doi/abs/10.1021/nn100563c

I performed the majority of experiments on the synthesis and characterization of the NCs. I wrote the manuscript draft.

Annex 9.

Lesnyak V., Wolf A., Dubavik A., Borchardt L., Voitekhovich S. V., Gaponik, N., Kaskel S., Eychmüller A.

3D assembly of semiconductor and metal nanocrystals: hybrid CdTe/Au structures with controlled content.

J. Am. Chem. Soc., **2011**, *133*, 13413–13420.

https://pubs.acs.org/doi/10.1021/ja202068s

I performed the majority of experiments on the synthesis, assembly, and characterization of the NCs. I wrote the manuscript draft.

Annex 10.

Wolf A., Lesnyak V., Gaponik N., Eychmüller A.

Quantum-dot-based (aero)gels: control of the optical properties.

J. Phys. Chem. Lett., **2012**, *3*, 2188–2193.

https://pubs.acs.org/doi/10.1021/jz300726n

I supervised the Bachelor project of André Wolf. I initiated this work and contributed to the experiments on the synthesis, assembly, and characterization of the NCs. I participated in discussions and writing of the manuscript. I am the corresponding author.

Annex 11.

Voitekhovich S. V., Lesnyak V., Gaponik N., Eychmüller A.

Tetrazoles: unique capping ligands and precursors for nanostructured materials.

Small, **2015**, *11*, 5728–5739.

https://onlinelibrary.wiley.com/doi/full/10.1002/smll.201501630

I contributed to writing of the review. I am one of the two corresponding authors.

Annex 12.

Dubavik A., Lesnyak V., Thiessen W., Gaponik N., Wolff T., Eychmüller A.

Synthesis of amphiphilic CdTe nanocrystals.

J. Phys. Chem. C, **2009**, *113*, 4748–4750.

https://pubs.acs.org/doi/10.1021/jp900140y

I co-supervised the PhD project of Aliaksei Dubavik. I initiated this work and contributed to the experiments on the synthesis and characterization of the NCs. I participated in discussions and writing of the manuscript.

Annex 13.

Dubavik A., Sezgin E., Lesnyak V., Gaponik, N., Eychmüller A.

Penetration of amphiphilic quantum dots through model and cellular plasma membranes.

ACS Nano, **2012**, *6*, 2150–2156.

https://pubs.acs.org/doi/abs/10.1021/nn204930y

I co-supervised the PhD project of Aliaksei Dubavik. I coordinated the experimental work and participated in discussions and writing of the manuscript. I am the corresponding author.

Annex 14.

Dubavik A., Lesnyak V., Gaponik N., Eychmüller A.

One-phase synthesis of gold nanoparticles with varied solubility.

Langmuir, **2011**, *27*, 10224–10227.

https://pubs.acs.org/doi/10.1021/la201638t r

I co-supervised the PhD project of Aliaksei Dubavik. I coordinated the experimental work and participated in discussions and writing of the manuscript. I am the corresponding author.

Annex 15.

Saldanha P. L., Brescia R., Prato M., Li H., Povia M., Manna L., Lesnyak V.

Generalized one-pot synthesis of copper sulfide, selenide-sulfide, and telluride-sulfide nanoparticles.

Chem. Mater., **2014**, *26*, 1442–1449.

https://pubs.acs.org/doi/10.1021/cm4035598

I co-supervised the PhD project of Pearl L. Saldanha. I contributed to experiments on the synthesis and characterization of the NCs. I also coordinated the experimental work and participated in discussions and writing of the manuscript. I am the corresponding author.

Annex 16.

Saldanha P. L., Lesnyak V., Manna L.

Large scale syntheses of colloidal nanomaterials.

Nano Today, **2017**, *12*, 46–63.

https://www.sciencedirect.com/science/article/abs/pii/S1748013216303322

I contributed to writing of the review. I am the corresponding author.

Annex 17.

Lesnyak V., Brescia R., Messina G. C., Manna L.

Cu vacancies boost cation exchange reactions in copper selenide nanocrystals.

J. Am. Chem. Soc., **2015**, *137*, 9315–9323.

https://pubs.acs.org/doi/10.1021/jacs.5b03868

I performed the majority of experiments on the synthesis and characterization of the NCs. I wrote the manuscript draft. I am one of the two corresponding authors.

Annex 18.

Lesnyak V., George C., Genovese A., Prato M., Casu A., Ayyappan S., Scarpellini A., Manna L.

Alloyed copper chalcogenide nanoplatelets via partial cation exchange reactions.

ACS Nano, **2014**, *8*, 8407–8418.

https://pubs.acs.org/doi/10.1021/nn502906z

I performed the majority of experiments on the synthesis and characterization of the NCs. I wrote the manuscript draft. I am the corresponding author.

Annex 19.

Vikulov S., Di Stasio F., Ceseracciu L., Saldanha P. L., Scarpellini A., Dang Z., Krahne R., Manna L., Lesnyak V.

Fully Solution-processed conductive films based on colloidal copper selenide nanosheets for flexible electronics.

Adv. Funct. Mater. **2016**, *26*, 3670–3677.

https://onlinelibrary.wiley.com/doi/full/10.1002/adfm.201600124

I co-supervised the PhD project of Sergey Vikulov. I contributed to experiments on the synthesis and characterization of the NCs. I also coordinated the experimental work and participated in discussions and writing of the manuscript. I am the corresponding author.

Annex 20.

Akkerman Q. A., Genovese A., George C., Prato M., Moreels I., Casu A., Marras S., Curcio A., Scarpellini A., Pellegrino T., Manna L., Lesnyak V.

From binary Cu_2S to ternary Cu-In-S and quaternary Cu-In-Zn-S nanocrystals with tunable composition via partial cation exchange.

ACS Nano, **2015**, *9*, 521–531.

https://pubs.acs.org/doi/10.1021/nn505786d

I supervised the Erasmus project of Quinten A. Akkerman. I contributed to experiments on the synthesis and characterization of the NCs. I also coordinated the experimental work and participated in discussions and writing of the manuscript. I am the corresponding author.

Annex 21.

Lox J. F. L., Dang Z., Dzhagan V. M., Spittel D., Martin-Garcia B., Moreels I., Zahn D. R. T., Lesnyak V.

Near-infrared Cu-In-Se-based colloidal nanocrystals via cation exchange.

Chem. Mater. **2018**, *30*, 2607–2617.

https://pubs.acs.org/doi/10.1021/acs.chemmater.7b05187

I co-supervise the PhD project of Josephine F. L. Lox. I coordinated the experimental work and participated in discussions and writing of the manuscript. I am the corresponding author.

Annex 22.

Gariano G., Lesnyak V., Brescia R., Bertoni G., Dang Z., Gaspari R., De Trizio L., Manna L.

Role of the crystal structure in cation exchange reactions involving colloidal Cu_2Se nanocrystals.

J. Am. Chem. Soc. **2017**, *139*, 9583–9590.

https://pubs.acs.org/doi/abs/10.1021/jacs.7b03706

I contributed to experiments on the synthesis and characterization of the NCs and participated in discussions and writing of the manuscript.

Annex 23.

Slejko E. A., Sayevich V., Cai B., Gaponik N., Lughi V., Lesnyak V., Eychmüller A.

Precise engineering of nanocrystal shells via colloidal atomic layer deposition.

Chem. Mater. **2017**, *29*, 8111–8118.

https://pubs.acs.org/doi/abs/10.1021/acs.chemmater.7b01873

I supervised the Erasmus project of Emanuele A. Slejko. I coordinated the experimental work and participated in discussions and writing of the manuscript. I am the corresponding author.

Annex 24.

Hendel T., Lesnyak V., Kühn L., Herrmann A.-K., Bigall N. C., Borchardt L., Kaskel S., Gaponik N., Eychmüller A.

Mixed aerogels from Au and CdTe nanoparticles.

Adv. Funct. Mater., **2013**, *23*, 1903–1911.

https://onlinelibrary.wiley.com/doi/full/10.1002/adfm.201201674

I contributed to experiments on the synthesis, assembly and characterization of the NCs, and participated in discussions and writing of the manuscript.

Annex 25.
Chen H., Lesnyak V., Bigall N. C., Gaponik N., Eychmüller A.
Self-assembly of TGA-capped CdTe nanocrystals into three-dimensional luminescent nanostructures.
Chem. Mater., **2010**, *22*, 2309–2314.
https://pubs.acs.org/doi/10.1021/cm9032572
I contributed to experiments on the synthesis, assembly and characterization of the NCs, and participated in discussions and writing of the manuscript.

Annex 26.
Sayevich V., Cai B., Benad A., Haubold D., Sonntag L., Gaponik N., Lesnyak V., Eychmüller A.
3D Assembly of all-Inorganic colloidal nanocrystals into gels and aerogels.
Angew. Chem. Int. Ed. **2016**, *55*, 6334–6338.
https://onlinelibrary.wiley.com/doi/full/10.1002/anie.201600094
I initiated this work, coordinated the experiments, and participated in discussions and writing of the manuscript. I am the corresponding author.

Annex 27.
Lesyuk R., Cai B., Reuter U., Gaponik N., Popovych D., Lesnyak V.
Quantum-dot-in-polymer composites via advanced surface engineering.
Small Methods **2017**, *1*, 1700189.
https://onlinelibrary.wiley.com/doi/full/10.1002/smtd.201700189
I supervised the Dresden Fellowship project of Dr. Rostyslav Lesyuk. I coordinated the experimental work and participated in discussions and writing of the manuscript. I am the corresponding author.

Annex 28.
Llorente Benavente V., Dzhagan V. M., Gaponik N., Iglesias R. A., Zahn D. R. T., Lesnyak V.
Electrochemical tuning of localized surface plasmon resonance in copper chalcogenide nanocrystals.
J. Phys. Chem. C 2017, *121*, 18244–18253.
https://pubs.acs.org/doi/abs/10.1021/acs.jpcc.7b05334
I supervised the DAAD Germany short research stay project ALERG of Victoria Benavente Llorente. I coordinated the experimental work and participated in discussions and writing of the manuscript. I am the corresponding author.

Annex 29.
Hosseinpour Z., Scarpellini A., Najafishirtari S., Marras S., Colombo M., Alemi A., Volder M. D., George C., Lesnyak V.
Morphology-dependent electrochemical properties of CuS hierarchical superstructures.
ChemPhysChem, **2015**, *16*, 3418–3424.
https://chemistry-europe.onlinelibrary.wiley.com/doi/full/10.1002/cphc.201500568
I initiated this work, coordinated the experiments, and participated in discussions and writing of the manuscript. I am one of the two corresponding authors.